Design and Performance of a Long, Over-Water Microwave Radio Link

J. E. Farrow

CONTENTS

LIST OF FIGURES

LIST OF TABLES

DESIGN AND PERFORMANCE OF A LONG, OVER-WATER MICROWAVE RADIO LINK

J. E. Farrow*

This paper discusses the design and the measured performance of a 76.8-km (47.7-mi) over-water 2.3 GHz microwave radio link. Since one of the terminals was located on an ocean tower, the maximum antenna height at that location was restricted to 49 m (160 ft). A 367-m (1200-ft) tower was used at the shore end to provide ray path clearance for normal and extreme refractivity gradients. The tower at the shore end supported antennas at 361 m (1180 ft), 345 m (1128 ft), 229 m (750 ft), and 49 m (160 ft) to provide quadruple diversity protection. Received signal level measurements were made over the link for several months including some of the summer period. Propagation performance of the link during this period was satisfactory.

Key words: 2 GHz propagation; long, over-water path; quadruple diversity performance analysis; refractive gradient analysis

1. INTRODUCTION

This long, over-water link supports the operation of the U.S. Navy's Charleston Tactical Air Crew Training System (TACTS) located off the coast of Georgia, south of Savannah. It connects a group of off-shore communication platforms with the land communication links at Shellman Bluff, GA, which carry the information signal to the Marine Corps Air Station at Beaufort, SC. The Naval Air Test Center at Patuxent River, MD, requested the aid of the Institute for Telecommunication Sciences (ITS) in designing a link-diversity structure that would meet the Defense Communications Agency reliability requirements for digital traffic to be carried over the link [Kirk and Osterholz, 1976]. The considerations submitted to the Navy are outlined in the Appendix. The Institute was then asked to assist the Navy in validating a contractor's suggested implementation, and then to consult with the Navy in evaluating the actual link performance.

2. DESCRIPTION OF THE LINK

This microwave radio link at the Charleston TACTS range provides a 6 Mb/s connection between an ocean tower and the shore facilities. It operates in the 1.7-to-2.4 GHz Government band allocated to fixed point-to-point service. This frequency band was chosen since the rain attenuation at these frequencies will not be a limiting factor in link reliability [Crane, 1980]. Although the link is only 76.8 km (47.7 mi) long, the height restriction on the ocean tower antenna required a 367-m (1200-ft) tower at Shellman Bluff to provide adequate path clearance. Since the link is over water and since such an asymmetrical

antenna arrangement is necessary, special attention was paid to the design of the diversity scheme to assure propagation reliability.

2.1 The Area

Figure 1 is a map showing the general area of the link and its relationship to the coastline. Because the area of coastal Georgia has been used extensively as an experimental area to establish and validate propagation models, the area was known to provide a challenging environment for such a link. [Vigants, 1975; Barnett, 1979]. Other options for the link, such as underseas fiber optic cable, were considered, but the microwave radio option was chosen because it promised to provide nearly the required level of service (see Table A-4) at the most attractive cost. The lack of an intermediate relay site required that the Navy accept the 76.8-km link and devise an equipment configuration that would provide the propagation reliability desired.

2.2 The Profile and Link Antenna Layout

The link profile was easy to construct since the shore station has an altitude of 3 m (10 ft) and is within a few kilometers of the shoreline and the ocean tower is located in about 20 m (66 ft) of water. The profile diagram shown in Figure 2 includes the towers and the antenna locations. Note that for normal refractive conditions (k = 1.42) the bottom antenna is well below the radio horizon. The placement of the antennas reflects the same design philosophy used in the design of a Defense Communication System microwave link across the English Channel [Zebrovitz, 1975; Wortendyke et al., 1979]. The purpose of the physical arrangement in each case was to design around the known propagation features of the sea-land interface and over-water links to provide transmission continuity to the maximum extent possible.

Basically, the highest antenna was located to provide clearance over the curve of the Earth for as small an effective Earth's radius factor as possible. The second antenna was located 16 m (53 ft) below the top antenna to provide good space-diversity protection against correlated phase interference fading [Vigants, 1975]. The mid-level antenna was located to provide line-of-sight reception for normal conditions for widely spaced diversity reception, and the bottom-level antenna was located to take advantage of the signals propagated through surface atmospheric ducts [Dougherty, 1969].

2.3 Radio Equipment Used

The radio equipment selected for this link was commercial quality digital microwave transmitters and receivers with the exception of the receiver diversity combiners. To take full advantage of the elaborate diversity scheme, four-fold (quad) diversity combiners developed for use on tropospheric scatter systems were procured and installed. This combiner is of the type that selectively amalgamates the four IF signals (a quad diversity, equal gain, pre-detection combiner) in proportion to their individual signal-to-noise ratios to produce a single signal to deliver to the detector/demodulator. Such a device will produce very nearly the optimum signal-to-noise ratio from the combination of the four available signals [Brennan, 1959].

A 6.2-Mb/s traffic baseband and a 192-kb/s orderwire and control channel bit stream are combined in the radio, and this composite stream imposes

four-phase modulation on the carrier. This modulation scheme at this bit rate is expected to be relatively immune to the effects of amplitude nonlinearities that are caused by phase-interference fading [Hause, 1981]. Table 1 shows the contractor's calculations for link equipment requirements and the resulting propagation performance. The 45-dB dispersive fade margin shown in Table 1 supports this contention since a greater vulnerability to nonlinear fading would be reflected in a somewhat lower (30 to 40 dB) dispersive fade margin.

3. DATA GATHERED

The purposes for recording the received signal levels (RSL's) for this link were to validate the design of the diversity system and also to test the installation for acceptance by the Government. Although the diversity design and the guarantee of link performance were largely the responsibility of the Government, the contractor was responsible for the detailed design, procurement, and installation of the shore tower at Shellman Bluff and the installation and check-out of all communication equipment.

3.1 Recording Setup

Figure 3 is a diagram of the recording setup. The signals from the three highest antennas are amplified at the antennas (to overcome the high loss of the long transmission lines), and sent to a down-converter where the signal is mixed down to a 70 MHz IF and sent to the quadruple-diversity combiner. The recording apparatus coupled off a sample of each of these four 70-MHz signals and converted the power level of the individual IF signals to dc voltages to drive the strip-chart recorder. A time code was placed on one of the six channels of the recorder to mark hours and days. The levels of signal for each radio channel were calibrated using a signal generator to simulate the inputs.

3.2 Strip Charts

Data were recorded on the strip chart from March through May and again for 2 weeks in July. During this period, 1718 hours of data were recorded. The chart was run at 7.5 cm (3 in.) per hour so that a day's data was 1.8 m (6 ft), which provided excellent resolution for the fading data. Figures 8 through 12 show examples of the strip-chart records.

4. DATA ANALYSIS

4.1 Signal Level Calibrations

To determine the strength of the received signal level as a function of strip-chart trace deflection, it is necessary to inject known levels of rf power at some point into the receiver system to simulate actual received power and to note the resulting chart-trace deflection. The ideal location to inject this calibrating signal is at the input to the first device in the receiver chain that provides signal gain. This allows proper account to be taken of the fixed gains and losses in the system which should be quite constant with time. Unfortunately, this was not possible with the current measurements. The great height of the tower at the land end made it advantageous to place rf preamplifiers near the upper antennas to send an amplified signal down the
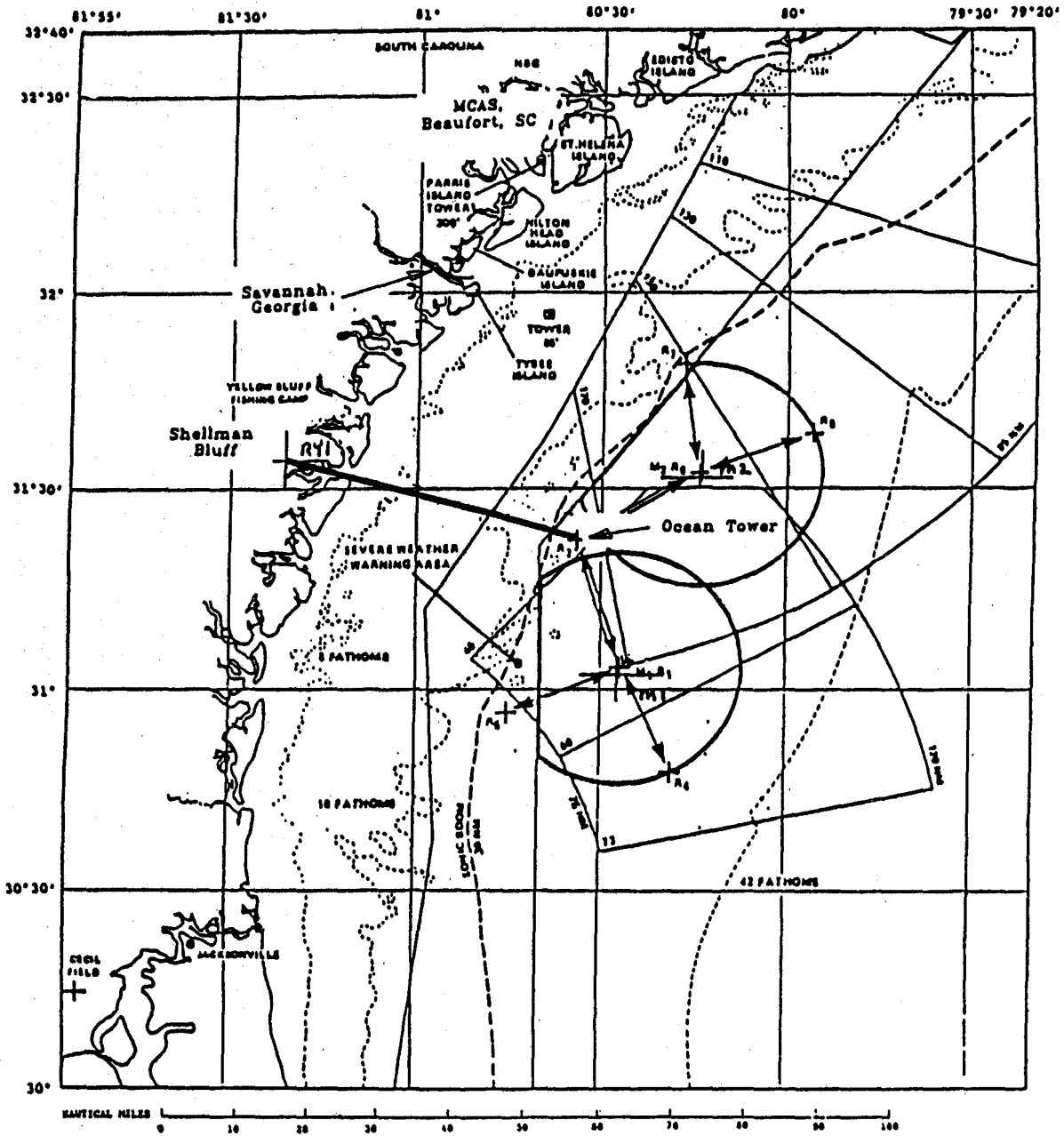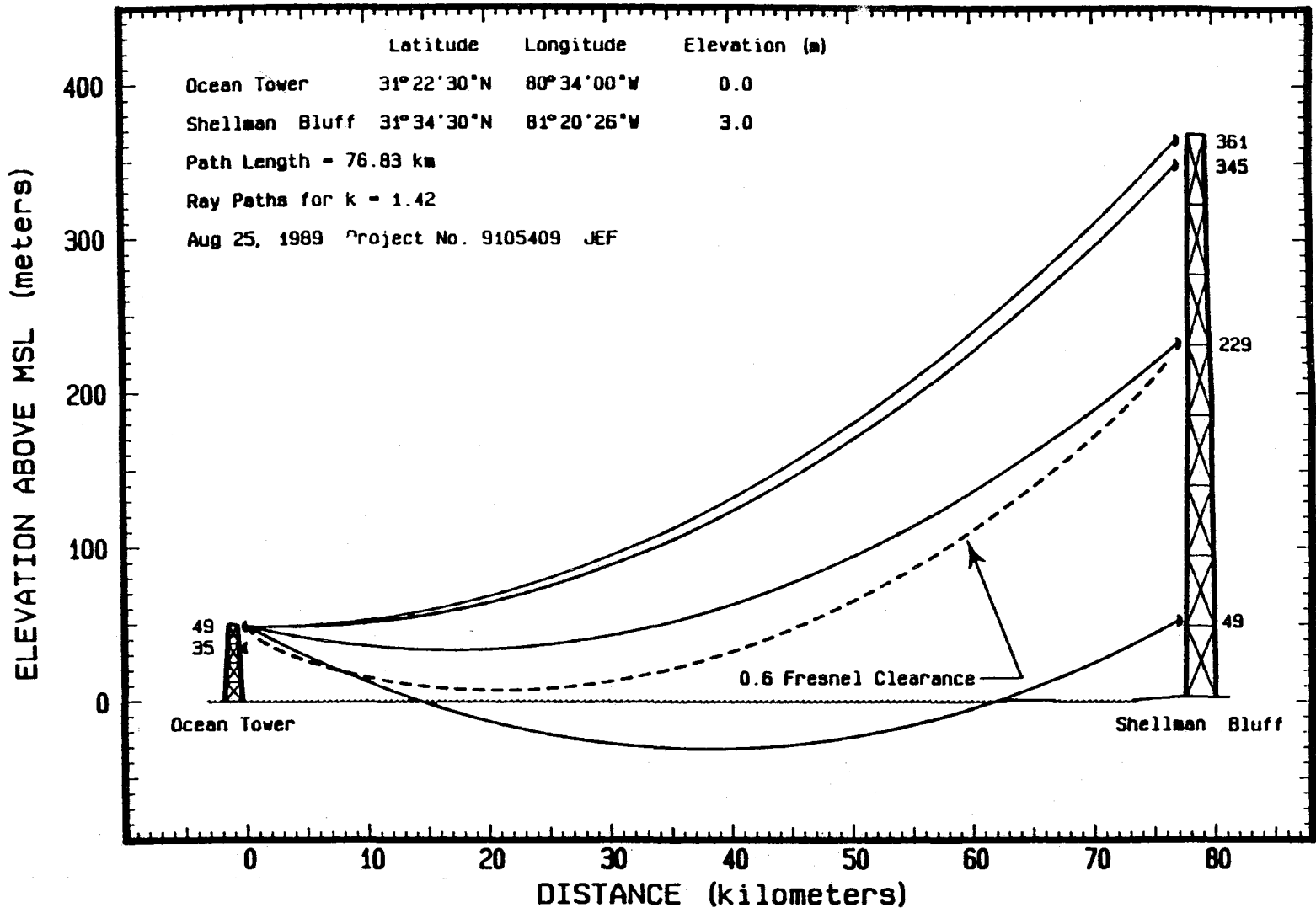
3

CHARLESTON TACTS

Figure 1. Plan view of the Shellman-Bluff-to-Ocean-Tower radio link.

Figure 2. Link diversity configuration.

tower. Calibrations were made using the measured parameters of gain and loss from the antenna systems. This lead to some inaccuracy in the calibrations. The inaccuracy in calibration, the narrow range of deflection, and the non-linearity of the calibrations makes detailed quantitative analysis of the time distribution of signal level impossible. There is a further difficulty with these calibrations, namely they were done only once at the start of the recording period. Experience has shown that some drift in gain through the rf chain will inevitably occur, and the calibration should be repeated periodically to correct for this effect. This was not possible for this test, but the drift over the period of measurement, which would be reflected in changes in the normal signal levels, did not seem to be sufficient to invalidate the analysis that was made of the data.

4.2 Propagation Regimes

During the course of the measurements, (which extended from early March intermittently until late July) at least five clearly distinct propagation regimes could be identified.

The first could be called the "normal line-of-sight" periods characterized by predicted median signal levels on the upper three antennas and a depressed level on the bottom antenna. The signals on the elevated antennas were observed occasionally to scintillate or to experience a few dB of random-appearing variation and, at other times, to have periods of deep phase-interference fading. This propagation mode would be characteristic of a path whose atmospheric conditions varied from well mixed to horizontally stratified.

A second regime is characterized by a strongly elevated signal on the bottom antenna and high median signal levels on the upper three antennas, usually with slow, deep fades. The deep fades on the signals on the upper three antennas during these periods were generally uncorrelated and a visual review of the chart showed no instance of deep fades occurring simultaneously on the upper three antennas. These periods are probably the result of moderate surface or low-level ducting which "guides" the signal to the lowest antenna and provides a source of multipath signals to cause the phase-interference fading on the upper three antennas.

A third regime is characterized by strong signals on the bottom antenna and severely depressed median signals on the upper three antennas. Signals on the upper antennas during these periods are also subject to rapid, deep fading, although, again, the fades are not highly correlated. These periods are probably the result of strong surface or low-level ducting that severely attenuates the signals at the upper three antennas and enhances the signal to the lower antenna.

A fourth regime is characterized by low signals on the top pair of antennas and on the bottom antenna but with a nearly normal line-of-sight level on the mid-level antenna. Such a pattern of signal levels could occur if an elevated duct were to attenuate the signals on the upper antennas while the lack of a lower level duct would allow the bottom antenna to receive the "normal" low-level diffraction signal.

A fifth regime is characterized by depressed signal levels on all antennas. Since this effect is rare, its cause may be one that occurs as a result of unusual circumstances. One possible scenario would involve a wedge-shaped, moist air mass that was being over-ridden by a much dryer layer so that signals from the ocean tower would be trapped and energy reaching any of the
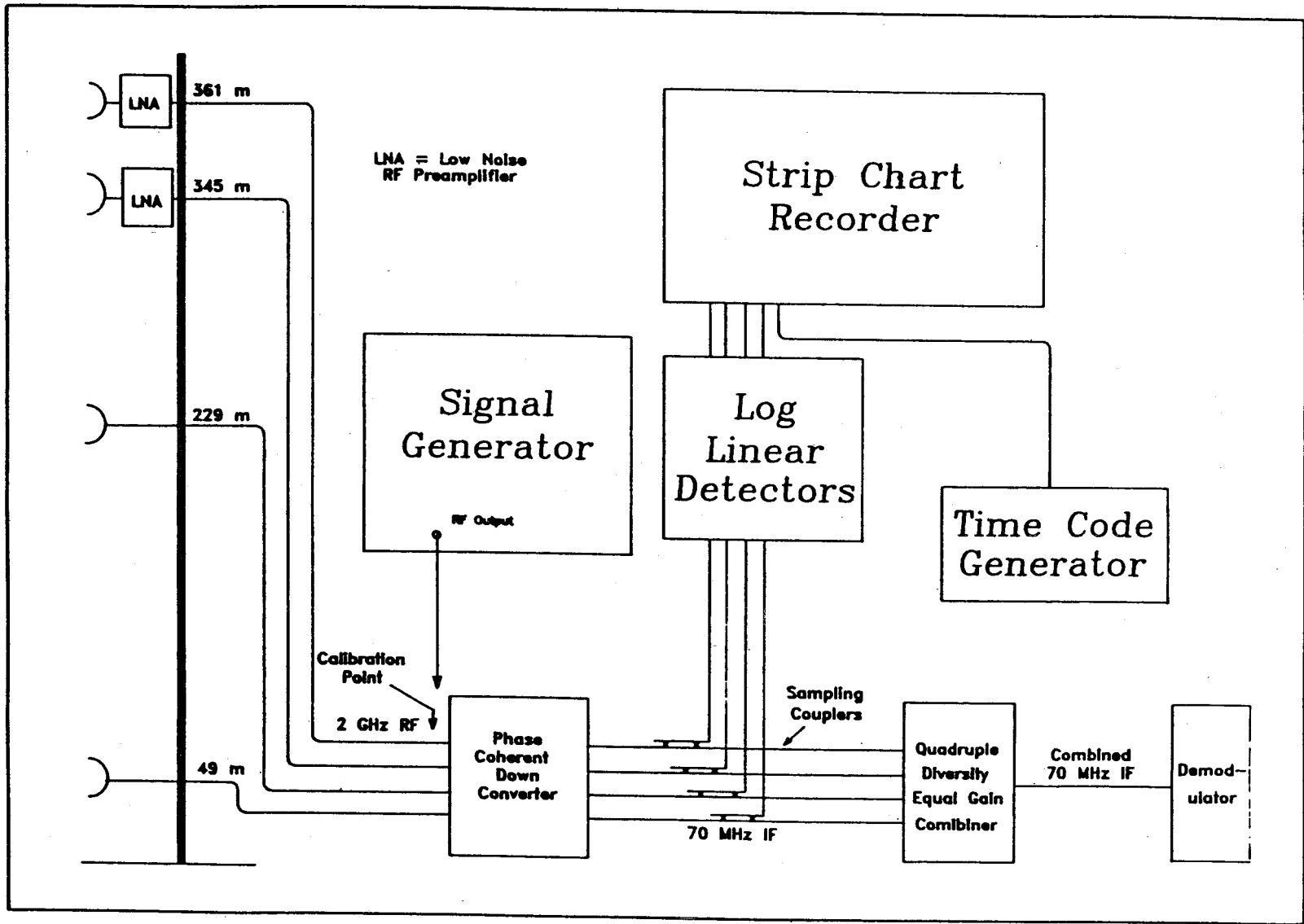
Figure 3. Link received signal level recording setup.

four shore-based antennas would be severely attenuated. Since this cause of the low-signal condition would be a fairly rapid, dynamic change in weather conditions, such a state of affairs would not be expected to last very long. The brevity of the periods during which RSL's in regime 5 were observed (Figure 4) supports this thesis. This is fortunate because such conditions, resulting in decreased signal levels on all diversity branches, seriously compromise overall link reliability.

Examples of each of these conditions are shown in Figures 4 through 8 in Section 5.3.

4.3 Analyzing the Strip Charts

Since the strip charts were automatically marked with hour and day signals, the first step in the analysis was to time and date the charts. Periods with no data were noted and during periods of good data, dates and times were written on the time channel. The smallest time division of analysis was one clock hour, since all occurrences of interest were this period or longer and since more rapid changes were considered to be part of one of the propagation regimes. Each hour of valid data was categorized into one of the five defined regimes and the results are presented by month so that seasonal effects can be observed.

5. PRESENTATION

5.1 Comparison of Predicted and Measured Signal Level Data

The single most significant indicator of the quality of the installation of a microwave link is the comparison of the expected received signal level with the observed signal level. Although this comparison tells nothing about the precision with which the input traffic signal is reproduced at the output, it does ensure that the basic structures of the link have been put into place correctly. Table 1 shows this information for the Shellman Bluff - Ocean Tower link. Note that this prediction is for clear line-of-sight propagation and thus is valid only for those periods when each antenna is in that mode. The strip chart sample in Figure 8 shows that the two highest antennas operate at or near this level, -46 dBm, when their signals are constant, indicating normal line-of-sight conditions. For the middle antenna, the signal level appears to be somewhat lower than the -46 dBm predicted, but this may be a result of the calibration uncertainty or of the drift in system gain in this receiver chain. At times, the highest level observed for this antenna, indicating line-of-sight propagation conditions, is above the -50 dBm level while other periods show a signal between -55 and -60 dBm. For the bottom antenna, the highest RSL observed exceeds the top calibration at -60 dBm, while the lowest level is below receiver noise level.

The signal levels on the highest pair of antennas on this link correlate well with the expected value, indicating that the antennas are properly oriented and that the installation is sound. The signal on the mid-level antenna appears to be somewhat below that expected during line-of-sight conditions for this antenna. The level shows fairly large changes from time to time, so there is no definite indication of antenna misalignment. The signal on the bottom antenna behaves as expected, changing from a level typical of a high-loss diffraction mode of propagation to a level typical of a much lower loss ducting mode.

Table 1. Summary of Predicted Link Performance

	Shellman Bluff		Ocean Tower
Frequency		2.3 GHz	
Path length		76.83 km (47.3 miles)	
Free space loss		137.3 dB	
Transmission line length	361 m		49 m
Transmission line loss	14.2 dB (-10 db RF preamp gain)		1.92 dB
Combiner losses	3 dB		2 dB
Other losses	1 dB		1 dB
Total fixed loss	8.2 dB		4.92 dB
Total loss		150.5 dB	
Antenna Diameter	3.05 m		2.45 m
Antenna Gain	34.7 dB		32.8 dB
Total Antenna Gain		67.5 dB	
Net path loss		82.9 dB	
Transmitter output power		37 dBm	
Received signal level		-45.9 dBm	
Threshold of performance		-86 dBm	
Thermal fade margin		40.1 dB	
Interference fade margin		65 dB	
Dispersive fade margin		45 dB	
Effective fade margin		38.5 dB	

Table 2. Signal Level Regimes by Fraction of Time

Month \ Regime	1	2	3	4	5
March	.619	.360	.011	.003	.007
April	.312	.668	.004	.016	0
May	.394	.561	0	.046	0
July	.823	.167	.010		
All Data	.505	.470	.006	.016	.003

5.2 Long Term Signal Level Effects

The observation of the signal-level performance during the spring and summer allows us to anticipate that the link will perform overall in such a way as to support the link traffic in an acceptable manner. Table 2 shows the fraction of the measurement period that the signal was in each of the five regimes. The most surprising aspect of this table is the large fraction of time that the lowest antenna received what approximates a line-of-sight signal level. Overall, for about half of the time (0.470), this antenna could have carried the traffic by itself. A heartening aspect of the table is the low fraction of time (0.003) during which all signals were severely depressed. Even during this time, all of the signals were not in deep fades simultaneously so the quadruple

diversity combining could have allowed the link to support traffic for a large part of these periods.

It is interesting to see the pattern suggested by the difference in periods during which low-level ducting (that is, regime 2) was observed in the various months. March showed about twice as much normal line-of-sight propagation as ducting while April showed twice as much ducting as normal line of sight. May also showed a preponderance of ducting but not so large as April, while July showed a smaller fraction of ducting periods than was observed in March. Apparently, the late spring - early summer period has much calmer winds or much longer periods of calm, leading to more and longer periods of well-developed atmospheric stratification than the earlier and later seasons.

Figures 4 through 8 show the changes of signal regime by the hour for the months of March, April, May, and July. The lowest trace is regime 1 and the highest is regime 5. Note how persistent the high signals are on the bottom antenna during the March-to-May time period--sometimes for days at a time, as shown by the appearance of the trace for regime 2 (the next one up from the bottom). These periods are much shorter during July.

5.3 Anecdotal Analysis

In this section, we will present examples of the various types of propagation described in Section 5.1. Typical chart samples are shown that are not unique but rather attempt to give an idea of the changeable conditions on the link.

Figure 8 shows an example of the most quiescent conditions on the link. All signals remain within a very narrow range of levels over a period of several hours. This is not a common occurrence, and indicates that ideal line-of-sight conditions exist. This signal level structure would indicate that no horizontal stratification of any intensity is present, and in fact, windy conditions would be expected to produce this effect. This period allows the normal levels of signal to be estimated. The signals from the upper two antennas are in the range of -46 dBm, the signal from the mid-level antenna is about 10 dB lower, and the signal from the bottom antenna is below -90 dBm.

The data sample in Figure 9 shows examples of regimes 1 and 2 and the rapidity of the transition between them. At 1200 on 4 April, the bottom antenna was operating in the high-loss diffraction mode and the upper antenna signals were fading moderately. Shortly before 1300, apparently a low-level layer formed, which increased the signal on the bottom antenna by more than 30 dB. Almost immediately, the signals on the top two antennas--and slightly later the signal on the mid-level antenna--began to exhibit the deep, slow fading caused by the arrival at the antenna of reflected and refracted secondary signals; these signals changed over periods of tens of minutes from being in phase conjunction to being in phase opposition with the main signal, leading to the 30-to-40-dB sharp bottom fades. The deep fades on the upper two antennas are almost always independent in time, the one exception in this figure occurring about 1545, when both signals decreased together. In this particular case, the level of signal on either the bottom or the mid-level antenna was sufficient to maintain service.

Figure 10 shows a condition that occurred fairly rarely (0.006 of the time) but could have reduced the availability of the link if the bottom antenna

March 1989

Propagation Regimes

Top Low / Mid Low / Bot Low

Top Low / Mid High / Bot Low

Top Low / Mid Low / Bot High

Top Med / Mid Med / Bot High

Top High / Mid High / Bot Low

No Data

5   10   15   20   25   30

Day of the Month
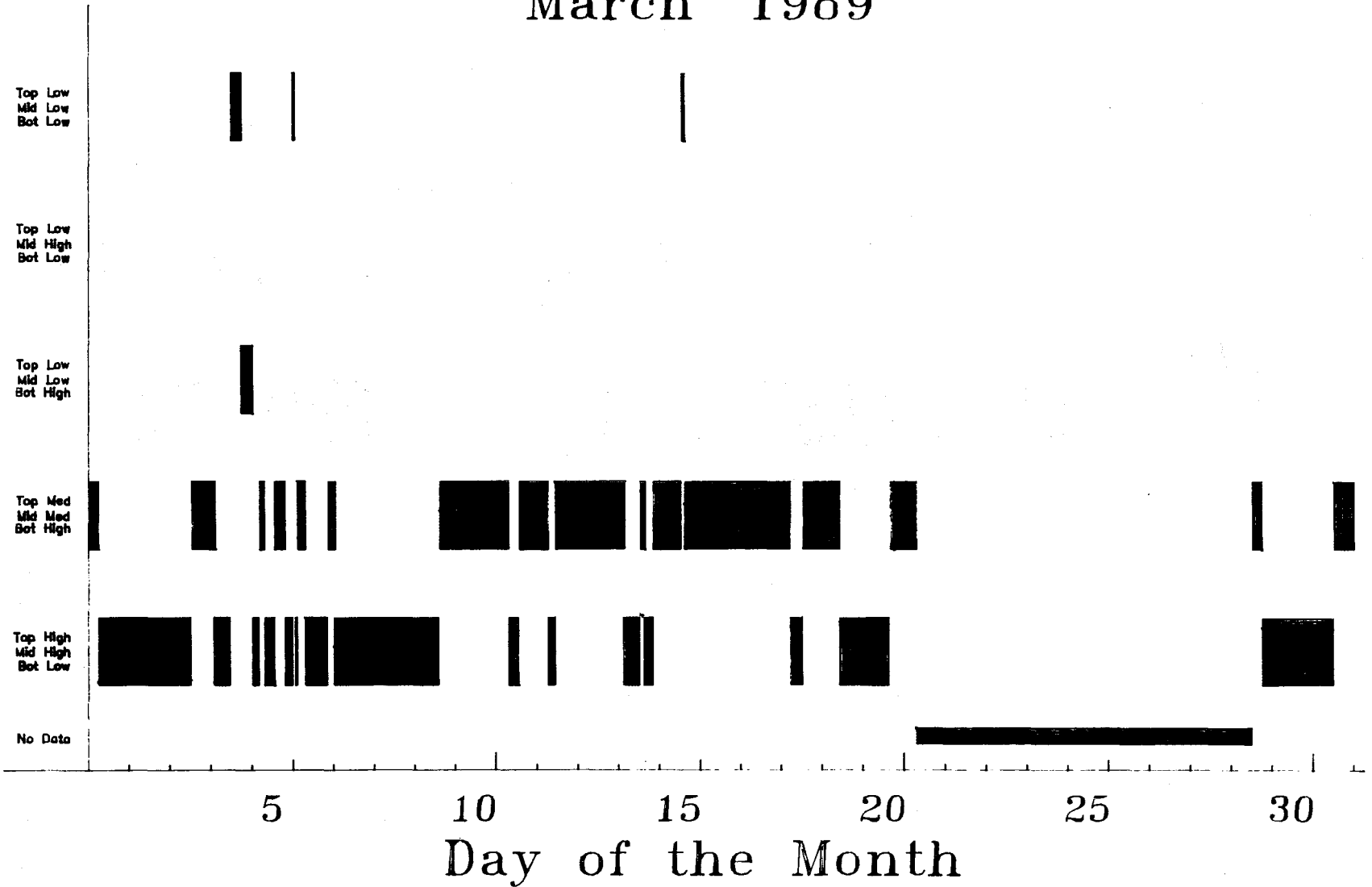
Figure 4. Propagation regimes by time, March 1989.
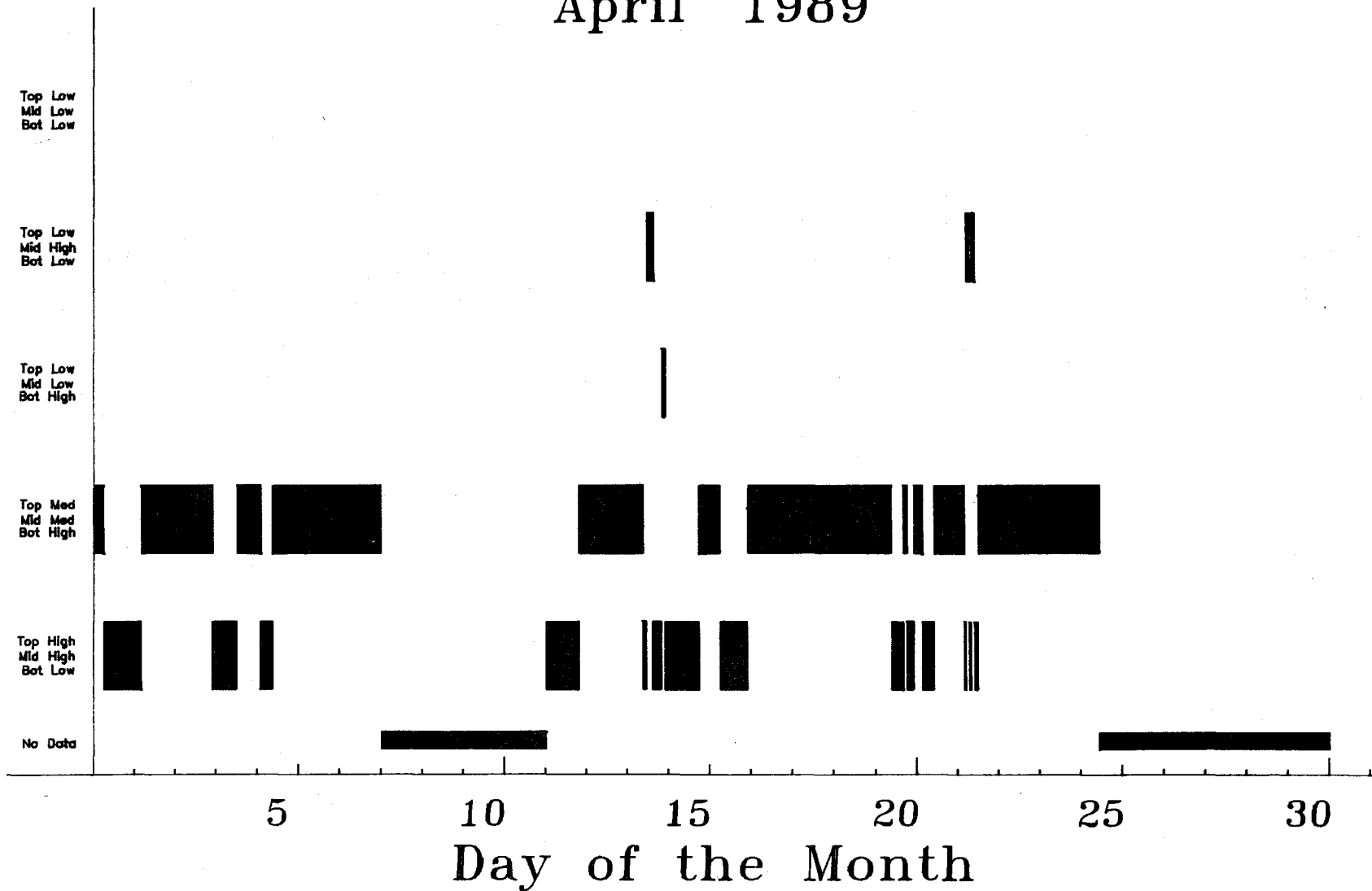
Figure 5. Propagation regimes by time, April 1989.
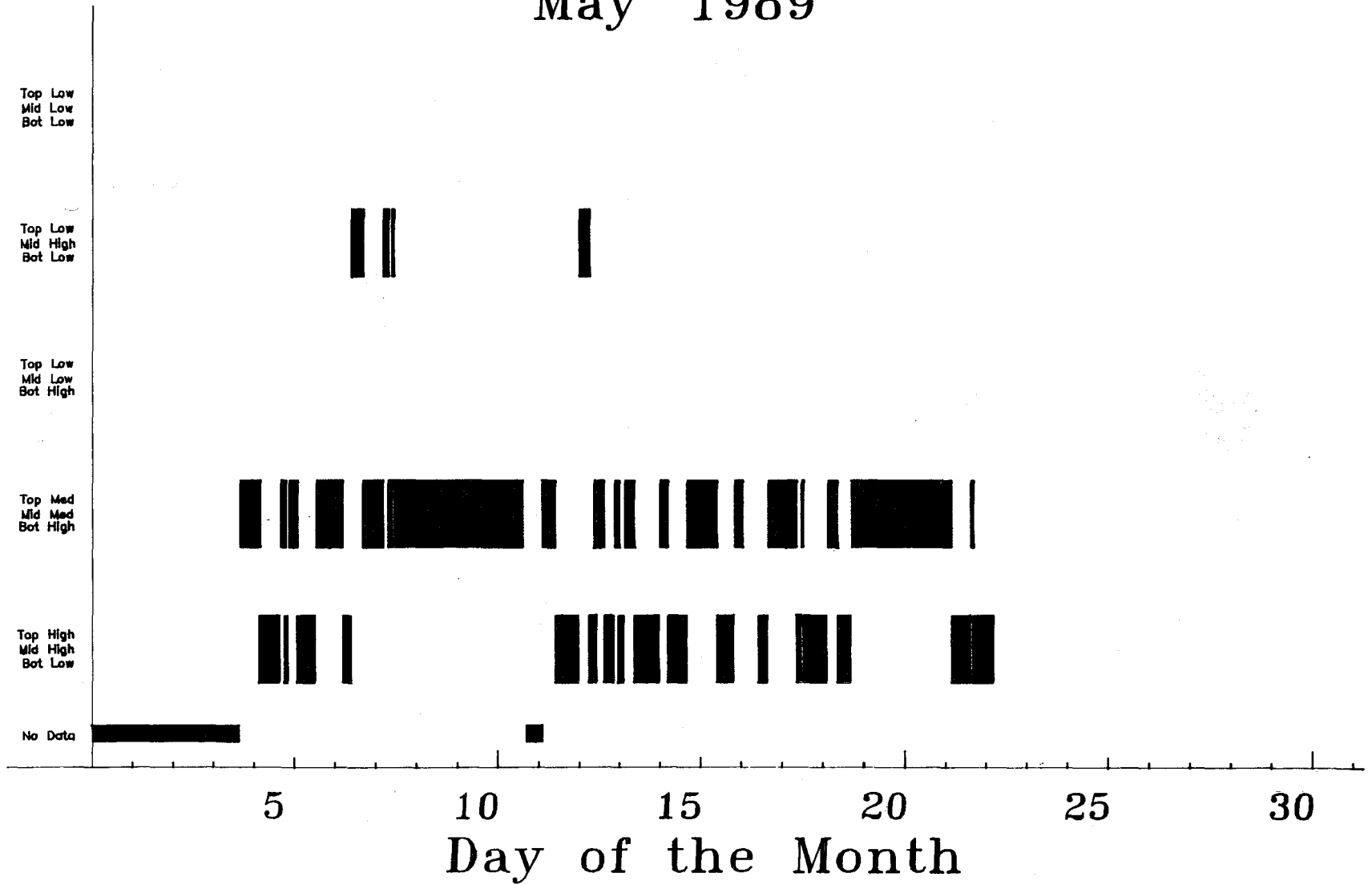
Figure 6. Propagation regimes by time, May 1989.

13
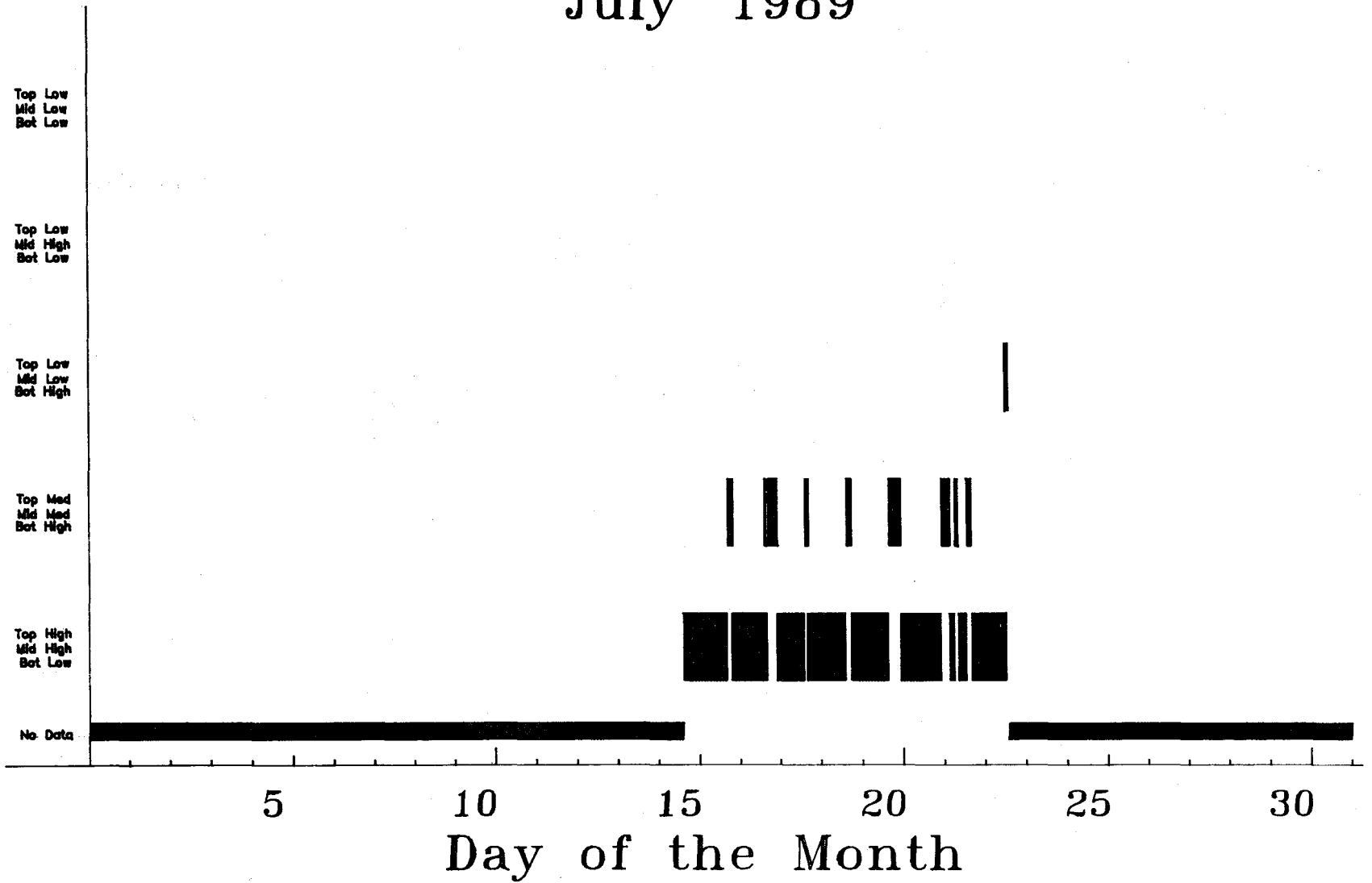
Figure 7. Propagation regimes by time, July 1989.
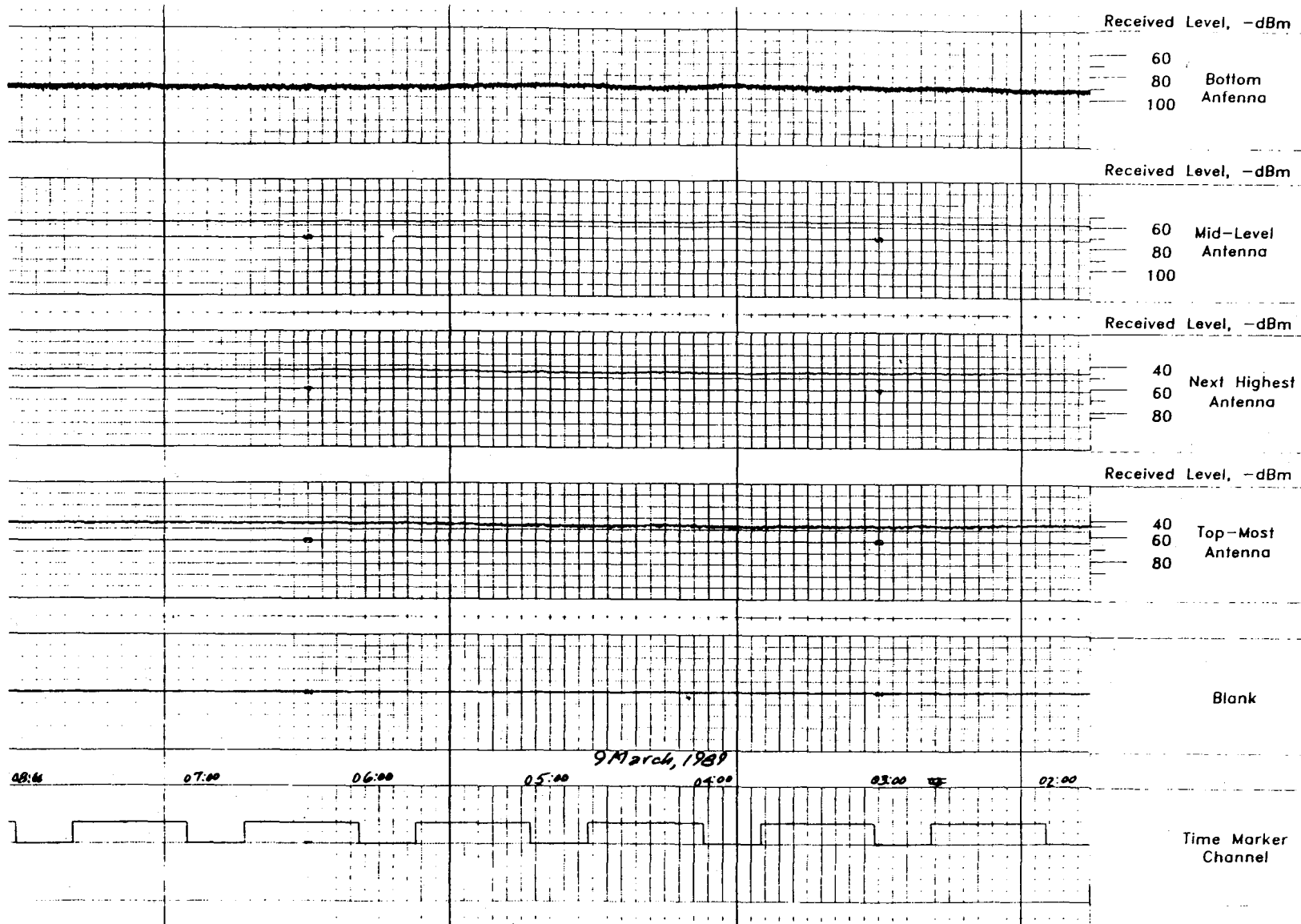
Figure 8. An example of quiescent propagation conditions, regime 1.

15
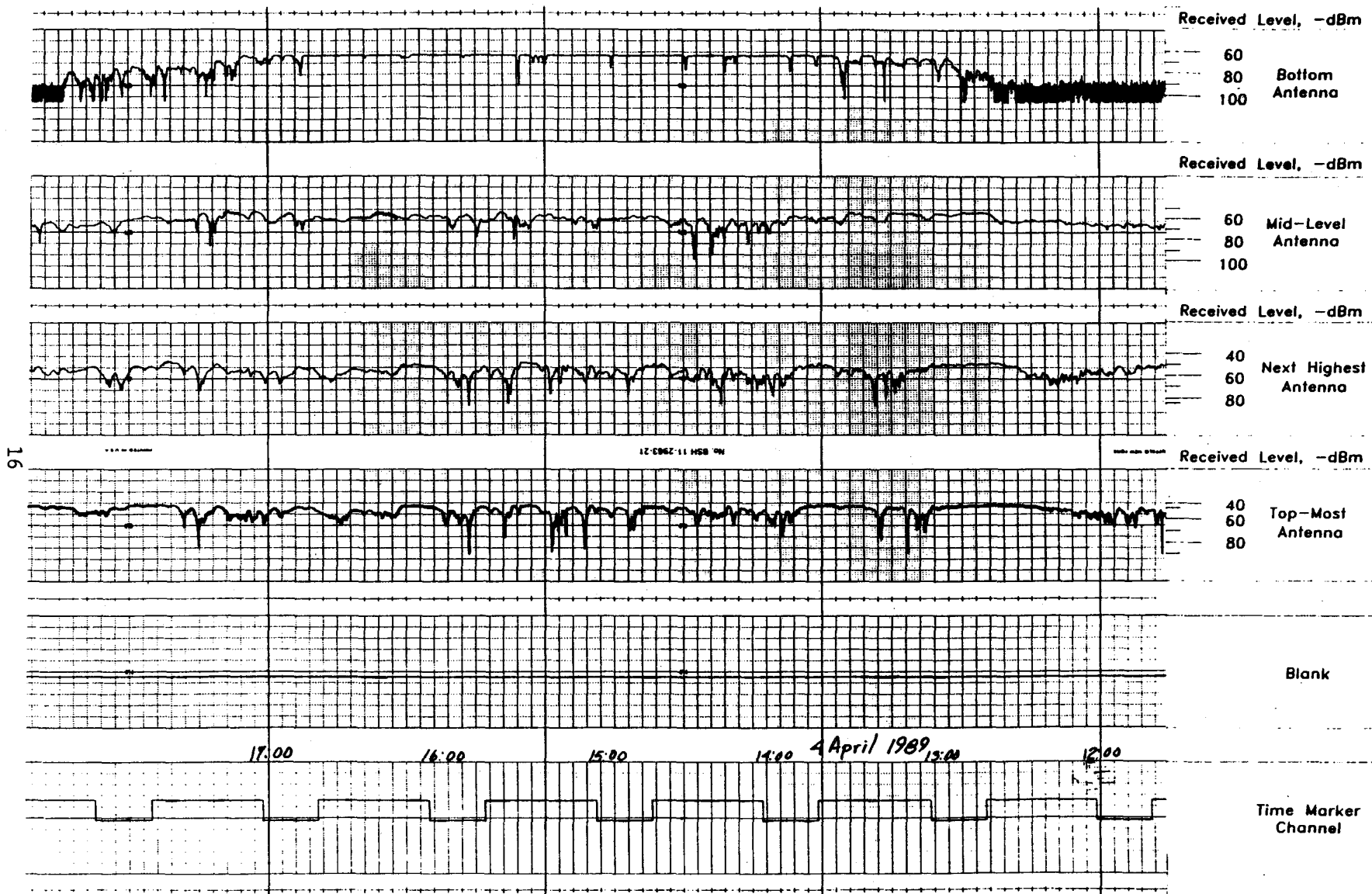
Figure 9. An example of the transition from propagation regime 1 to regime 2.

Received Level, −dBm

60
80   Bottom
100 Antenna

Received Level, −dBm

60   Mid−Level
80   Antenna
100

Received Level, −dBm

40   Next Highest
60   Antenna
80

Received Level, −dBm

40   Top−Most
60   Antenna
80

Blank

07:00   06:00   05:00   04:00   03:00   02:00

19 April, 1989

Time Marker
Channel

17
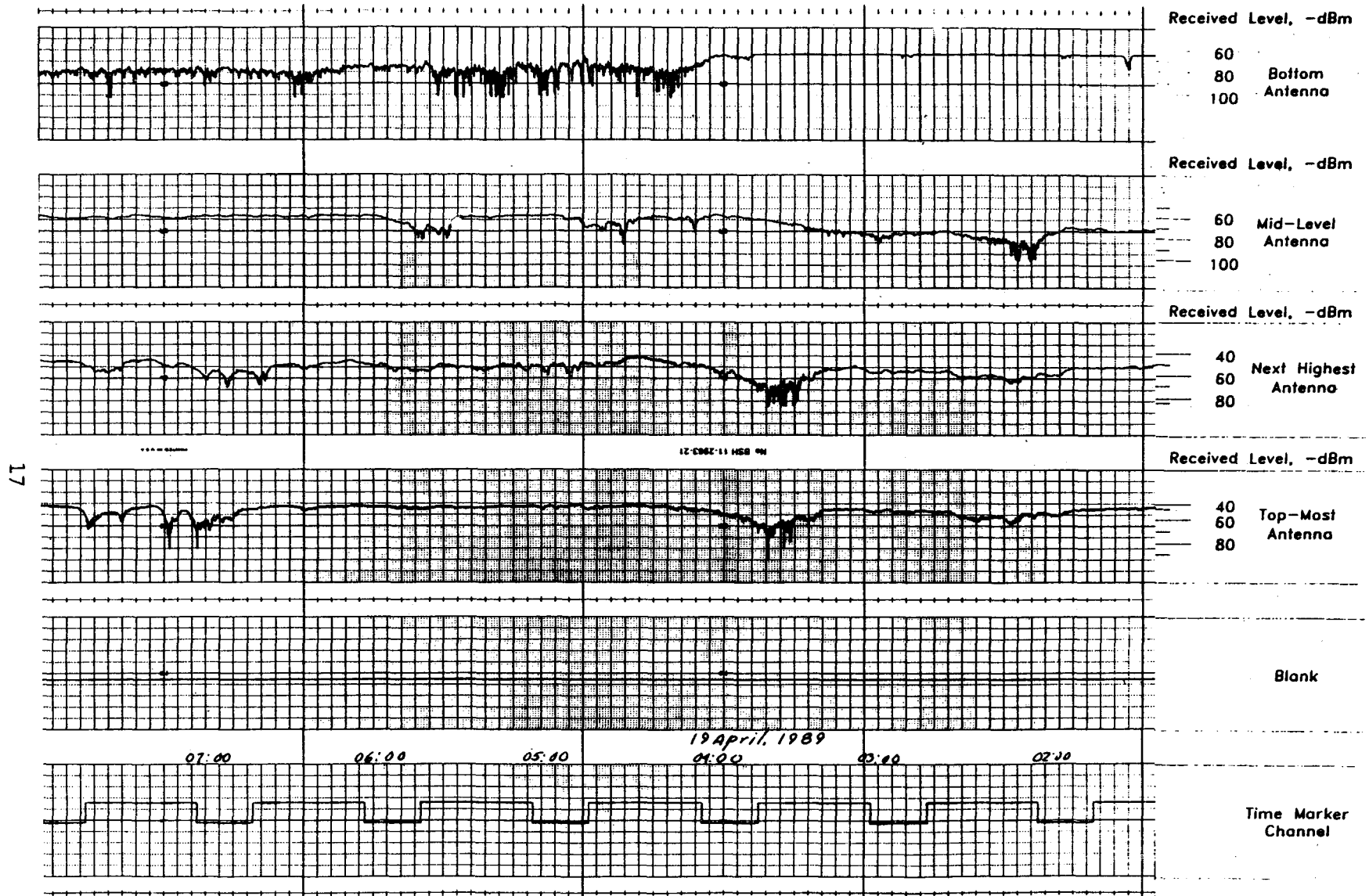
Figure 10.   Regime 3, bottom antenna showing the highest signal.

had not been installed. From about 0200 until 0400 on 19 April, the signals on the three highest antennas were significantly reduced below normal, while the bottom antenna's signal was quite high. Even though the signals on the upper three antenna's could have maintained service during this particular incident (from Table 1, note that the performance threshold is -86 dBm), this is a good indication of the efficacy of the diversity scheme.

Figure 11 illustrates the appearance of signals during regime 4 when signals were low on the top two antennas and on the bottom one but the mid-level antenna was maintaining a more normal level. From Table 2, this condition is observed for 0.018 of the time, so the diversity system is significantly improving link availability.

The condition shown in Figure 12 is the one that will cause the most serious decrease in link availability. During this and similar periods, the bottom antenna received very low "normal" signal while all three upper antennas simultaneously operated at seriously reduced levels. There is apparently no diversity arrangement that could provide protection during this sort of fade event. The link would not have been out of service for this entire period because the combiner would have added the signals for the best output on a continuing basis. It does not appear from a careful inspection of the chart that all signals fell below -86 dBm simultaneously for more than a small fraction of the entire period.

6. CONCLUSIONS AND RECOMMENDATIONS

Even though periods of low signal on all diversity branches were observed, these periods were short and the total time during which the link would have exhibited error rates in excess of 1 in 10^6 would be very short. This level of performance fully justifies the diversity design.

The link was installed properly, as far as can be determined from these measurements, and should continue to perform to the design level. The signal level on the mid-level antenna should be checked during the next preventive maintenance routine to determine if possible the reason for its apparent depression.

7. ACKNOWLEDGMENTS

The author wishes to acknowledge the support of Mr. Marvin Ranta of the Naval Air Test Center for his support of the project and Mr. John Meirose of NATC for assisting with the data collection effort. Thanks are also due Mr. Lauren Pratt of ITS for his effort in assembling the test equipment and setting up the measurements in the field.
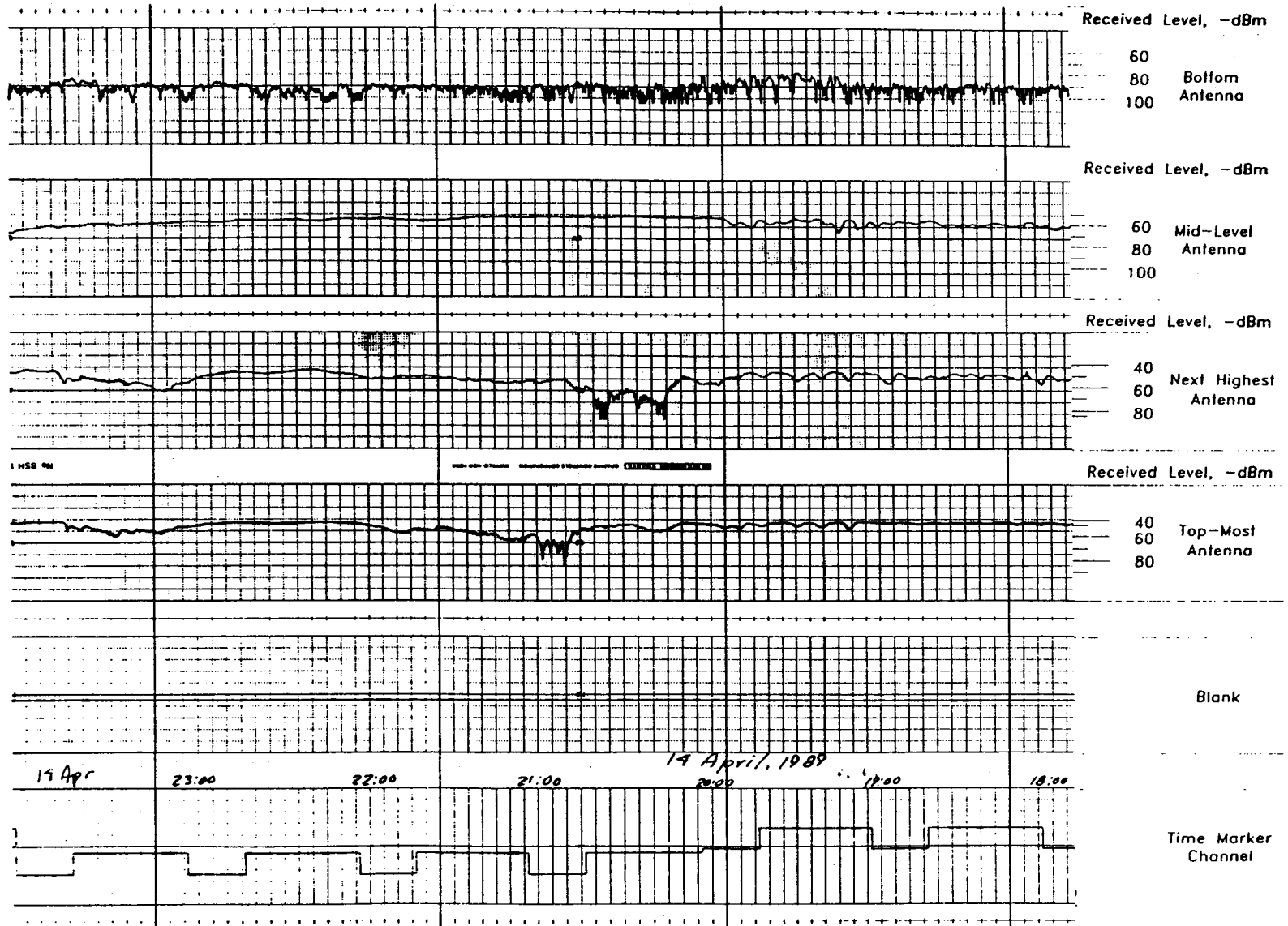
Figure 11. Regime 4, middle antenna showing the highest signal.
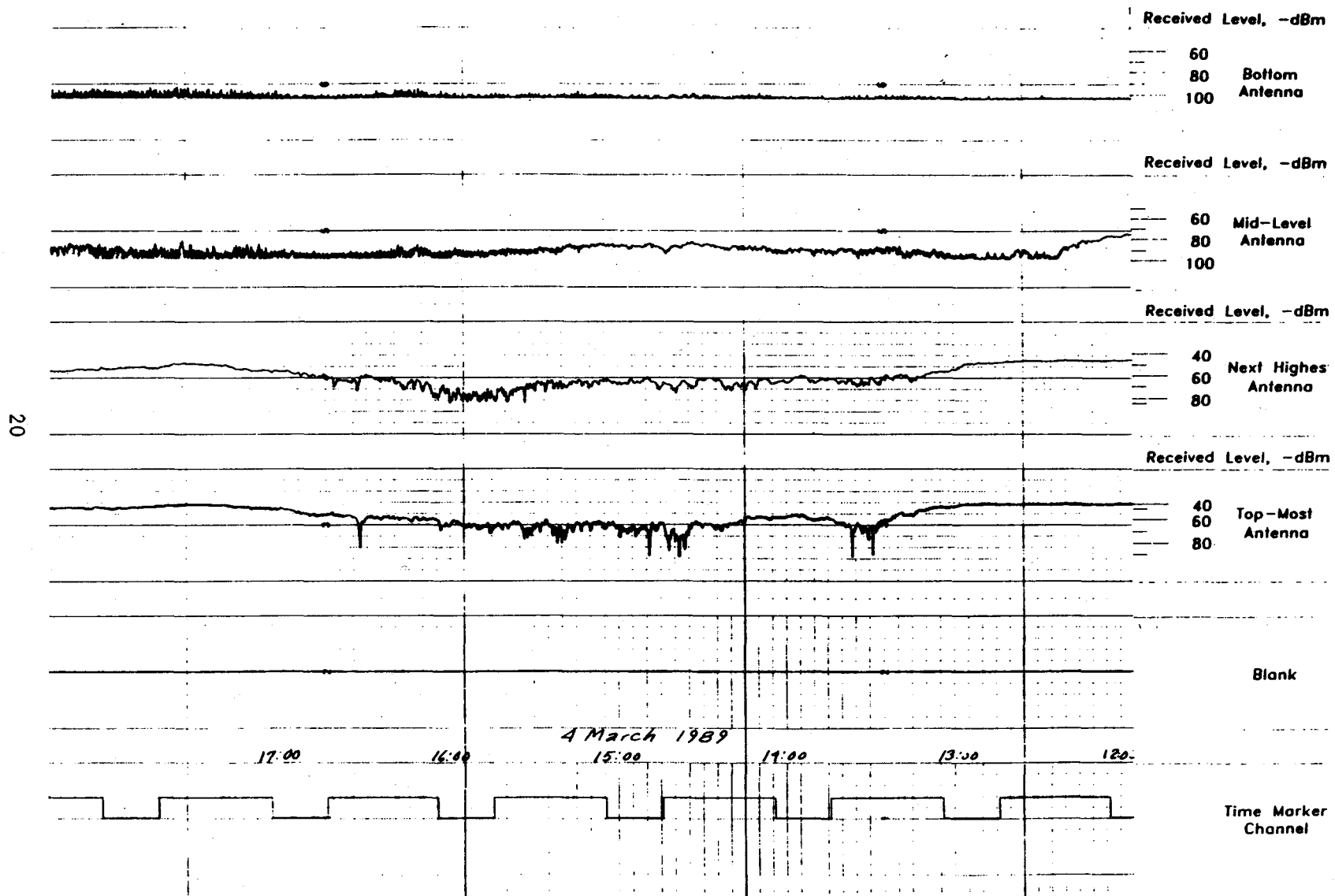
Figure 12. Regime 5, all antennas showing severely depressed levels.

20

8. REFERENCES

Barnett, W. P. (1979), Multipath fading effects on digital radio, IEEE Trans. Commun. COM-27, No. 12, December.

Brennan, D. G. (1959), Linear diversity combining techniques, Proc. IRE 47, No. 6, pp. 1075-1102.

Crane, R. K. (1980), Prediction of attenuation by rain, IEEE Trans. Commun. COM-28, No. 9, pp. 1717-1733.

Dougherty, H. T. (1969), A survey of microwave fading mechanisms, remedies and applications, ESSA Report ERL 69-WPL4. (NTIS Order No. COM-17-50288).

Hause, L. G. (1981), Selective fading on a long 8 GHz line-of-sight path in Europe, NTIA Report 81-84, September, 101 pp.

Kirk, K. W., and J. L. Osterholz (1976), DCS digital transmission system performance, Tech. Report 12-76, Defense Communication Engineering Center, 1860 Wiehle Ave., Reston, VA 22025.

Vigants, A. (1975), Space diversity engineering, Bell System Technical Journal 54, No. 1, January.

Wortendyke, D. R., A. P. Barsis, and R. R. Larsen (1979), Signal level distributions and fade event analyses for a 5 GHz microwave link across the English Channel, NTIA Report 79-30.

Zebrovitz, S. (1975), The use of multiple diversity to minimize the effects of ducting on a long microwave path, Proc. IEEE National Telecommun. Conf., October 23-28.

APPENDIX: LONG-TERM LINK RELIABILITY PREDICTIONS

During the design phase of this system, ITS assisted NATC in assessing various alternatives for this communication link. Two of these analyses are discussed here to provide background for the data collection and analysis. The first analysis considered the expected performance of a link over this path considering only the effects of rain attenuation and multipath fading. The second analysis considered the path as one subject to diffraction fading arising from the effects of sub-refractive conditions, as well as the effects of surface reflections.

A.1 The Rain Attenuation and Multipath Analysis

This analysis utilized a set of programs prepared at ITS [Hause, 1986] that have as inputs the geographic, physical, and climatological information about a proposed radio link and, based on a particular equipment selection, produce an expected distribution of single-receiver basic transmission loss and a receiver carrier-to-noise-ratio distribution. The path geometry and meteorological information input and the calculated outputs are shown in Table A-1. Table A-2 shows the inputs of the remaining meteorological parameters and the calculated basic transmission loss. Figure A-1 shows the profile on which these calculations were based. Note that the mid-level and bottom antennas are not considered in this analysis. Figure A-2 shows the distribution of transmission loss due to multipath effects based on the methods given in the International Radio Consultative Committee Recommendations [CCIR, 1982]. In order to develop a distribution of carrier-to-noise ratio, the effects of diversity gain and the effects of rain attenuation (which produce the same attenuation to the signal on all diversity branches of this link) must be considered. The method of calculating diversity improvement is from CCIR (1982), and rain attenuation is calculated for various fractions of the year by a method developed at ITS [Dutton, 1984]. Table A-3 gives the input parameters and the rain attenuation for various fractions of the year, and Table A-4 gives the output of the analysis. The calculated error-free-second availability is compared with the DCA requirement [Kirk and Osterholz, 1976], and although that requirement is not met, the link meets the design reliability of 0.99995 established by the Navy. Figure A-3 shows the carrier-to-noise distribution for the link. The results of these calculations indicate that the link will support the traffic with the desired reliability.

A.2 The Obstruction Fading Analysis

The effect of subrefractive atmospheric conditions on the performance of microwave links has been known for some time but recently, work has been undertaken to quantify these effects [Schiavone, 1981; Vigants, 1981]. These algorithms have been coded at ITS for the U.S. Army Information Command in a program called POMMP (Performance of Mixed-Mode Microwave Paths). The parameters necessary to operate the programs are given in Table A-7. The analysis takes into account measured information on the fraction of time that sub- and superrefractive conditions occur in a particular geographic area. The data needed to perform such an analysis are obtained from radio sonde readings, which measure air temperature, pressure, and relative humidity at intervals as the sonde is carried aloft on a balloon. These measurements are taken at fixed locations twice a day and, if the radio path to be analyzed is near such a

weather station, a time distribution of refractive gradient in the lower 500 m of atmosphere can be obtained. An example of this distribution for the Georgia coastal area taken from Samson (1975) is shown as Figure A-4. A technique developed by the author and Mr. Hause [Hause and Farrow, 1985] permits the reduction of these curves to a bi-modal distribution similar in effect to the method given by Schiavone (1981) to facilitate the analysis. Table A-8 gives the input parameters for the calculation as well as the resulting refractivity gradient distribution; Figure A-5 shows the calculated bi-modal distribution. As the refractive gradient changes from the normal level of -57 N-units per km of altitude (which corresponds to an equivalent Earth's radius factor, k, of 4/3) to 0 N-units per km (k = 1) and on to positive gradients of +157 N-units per km (k = 0.5) and more, the Earth can be visualized as "bulging" up toward, and finally into, the radio path. In the other direction, the k-factor increases without bound giving a "flat Earth", and for larger negative values, a concave Earth with a negative radius. The effect of Earth bulge is illustrated in the sequence in Figures A-6 through A-11. The basic transmission loss over a path depends on the clearance of the beam over the terrain, and the loss increases very rapidly as the clearance goes from positive to grazing incidence and then to negative clearance or obstruction. This increase in loss is shown in Figure A-12, which is the distribution of combined path loss, and in Table A-7, which shows the tabulation of the various components of loss.

A.3 Discussion

It is coincidental that both techniques for predicting the most severe attenuation over the path arrive at similar conclusions, since quite different methods of analysis are used. Comparison of the extreme attenuation exceeded for 0.00001 of the year (shown in the lower right-hand corner of each graph) on Figures A-2 and A-11 shows values of 186.5 dB and 181.5 dB respectively, with the lower value resulting from the multipath calculation. In interpreting these data, however, it must be understood that the multipath attenuation effects are susceptible to improvement by space or frequency diversity while the diffraction or "Earth-bulge" fading is not, which would indicate that link reliability will be limited by the system gain available to overcome the diffraction fading.

It is important to bear in mind that neither of these prediction techniques considers the contribution of the mid-level and bottom antennas to link availability, nor does either technique suggest the utility of the extreme diversity spacing used. As the measured data show, the bottom antenna can provide adequate signal to carry traffic during a considerable part of the time. The link design used in this case has evolved over a number of years from analyses of the performance of a number of links and considerations of atmospheric effects not addressed by the best currently available models. Even the mixed-mode prediction technique has an inherent assumption that the vertical gradient of refractive index is constant over the elevation through which the signal travels, and this is known not to be true for all periods of time and is probably untrue for most periods, as can be inferred from the data presented here. The standard prediction models perform well when they are used within their range of applicability, but must be used with caution when the limits are exceeded. Paths such as Shellman Bluff - Ocean Tower need the careful and individual engineering approach that the Naval Air Test Center took in this case.

The link design for this path was intended to be quite conservative and some cost was incurred by the installation of the lower two antennas and associated radio equipment. This incremental cost was not a large fraction of that of the total link installation, and the performance of the link is improved to a noticeable extent by the presence of these lower antennas.

A.4 References

CCIR (1982), Recommendations and Reports of the CCIR, 1982; Volume V; Propagation in non-ionized media, ITU, Geneva, Switzerland.

Dutton, E. J. (1984), Microwave terrestrial link rain attenuation prediction parameter analysis, NTIA Report 84-148, April, 194 pp. (NTIS Order No. PB 84-207984).

Hause, L. G., and J. E. Farrow (1985), Propagation predictions for marginal LOS microwave paths, Proc. 1985 IEEE Military Commun. Conf., Boston, MA, October 20-23, pp. 369-373.

Hause, L. G. (1986), Algorithms used in ARROWS: autodesign of radio relay optimum wideband systems, NTIA Report 86-207, October, 138 pp. (NTIS Order No. PB 87-126405/AS).

Kirk, K. W., and J. L. Osterholz (1976), DCS digital transmission system performance, Tech Report 12-76, Defense Communication Engineering Center, 1860 Wiehle Ave., Reston, VA 22025.

Samson, C. A. (1975), Refractivity gradients in the northern hemisphere, U.S. Department of Commerce, Office of Telecommunications, OT Report 75-59.

Schiavone, J. A. (1981), Prediction of positive refractivity gradients for line-of-sight microwave radio paths, Bell System Technical Journal 60, No. 6, Part 1, July-August.

Vigants, A. (1981), Microwave radio obstruction fading, Bell System Technical Journal 60, No. 6, Part 1, July-August.

Table A-1. Path Geometry Input and Calculation Output Table

Path Geometry and Meteorlogical Information
Ocean Tower R2 to Shore Tower

For the R2 RY1 Path

Path Length	(km)	76.8268
Carrier Frequency	(GHz)	2.0000000
Transmitting Primary Antenna Height Above Ground	(m)	47.244
Receiving Primary Antenna Height Above Ground	(m)	361.188
Mean Terrain Elevation	(m)	0.003
Standard Deviation of Elevations	(m)	0.058

Path Azimuths from True North:

R2 to RY1	(d/m/s)	286 58' 48.4"
RY1 to R2	(d/m/s)	106 34' 33.4"

Path Azimuths from Magnetic North:

R2 to RY1	(d/m/s)	286 58' 48.4"
RY1 to R2	(d/m/s)	106 34' 33.4"

Primary Antenna Values For Average Earth's Radius Factor:

Average Earth's Radius Factor		1.4159630
Transmitting Antenna Elevation Angle	(d/m/s)	-00' 26.7"
Receiving Antenna Elevation Angle	(d/m/s)	-28' 48.8"
Effective Path Length	(km)	76.8268
Minimum Ray Path Absolute Clearace Distance	(km)	2.0000
Minimum Ray Path Absolute Clearance	(m)	47.207
Minimum Ray Path 1st Fresnel Zone Clearance Distance	(km)	14.0000
Minimum Ray Path 1st Fresnel Zone Clearance	(1st Rad)	1.3599
Mean Atmospheric Pressure on the Ray Path	(kPa)	99.4350517
Mean Ray Path Height Above Ground	(m)	141.173

Primary Antenna Values For Extreme Subrefractive Earth's Radius Factor:

Extreme Subrefractive Earth's Radius Factor		0.6666667
Minimum Ray Path Absolute Clearance Distance	(km)	20.0000
Minimum Ray Path Absolute Clearace	(m)	-3.945
Minimum Ray Path 1st Fresnel Zone Clearance Distance	(km)	20.0000
Minimum Ray Path 1st Fresnel Zone Clearance	(1st Rad)	-0.084

General Link Information:

Estimated Annual Worst Month Average Snow Depth at R2	(m)	0.000
Estimated Annual Worst Month Average Snow Depth at RY1	(m)	0.000

Tree growth at R2 is estimated at 0.000 m per year.
Tree growth at RY1 is estimated at 0.000 m per year.

Table A-2. Meteorological Parameter and Basic Transmission Loss Output Table

19 May, 1986 Project:9105409 JEF

Median Basic Transmission Loss
Ocean Tower R2 to Shore Tower

Path 1 Ocean Tower R2 to Shore Tower

Path Length	(km)	76.827
Primary Frequency	(GHz)	2.0000
Average Summer Temperture	(Celsius)	26.7
Mean Path Pressure	(kPa)	99.4351
Absolute Humidity	(gm/cu. m)	18.00
Oxygen Absorption	(dB)	0.424
Water-Vapor Absorption	(dB)	0.035
Total Atmospheric Absorption	(dB)	0.459
Free Space Basic Transmission Loss	(dB)	136.181
Total Path Median Basic Transmission Loss	(dB)	136.640

19 May, 1986 Project No. 9105409 JEF
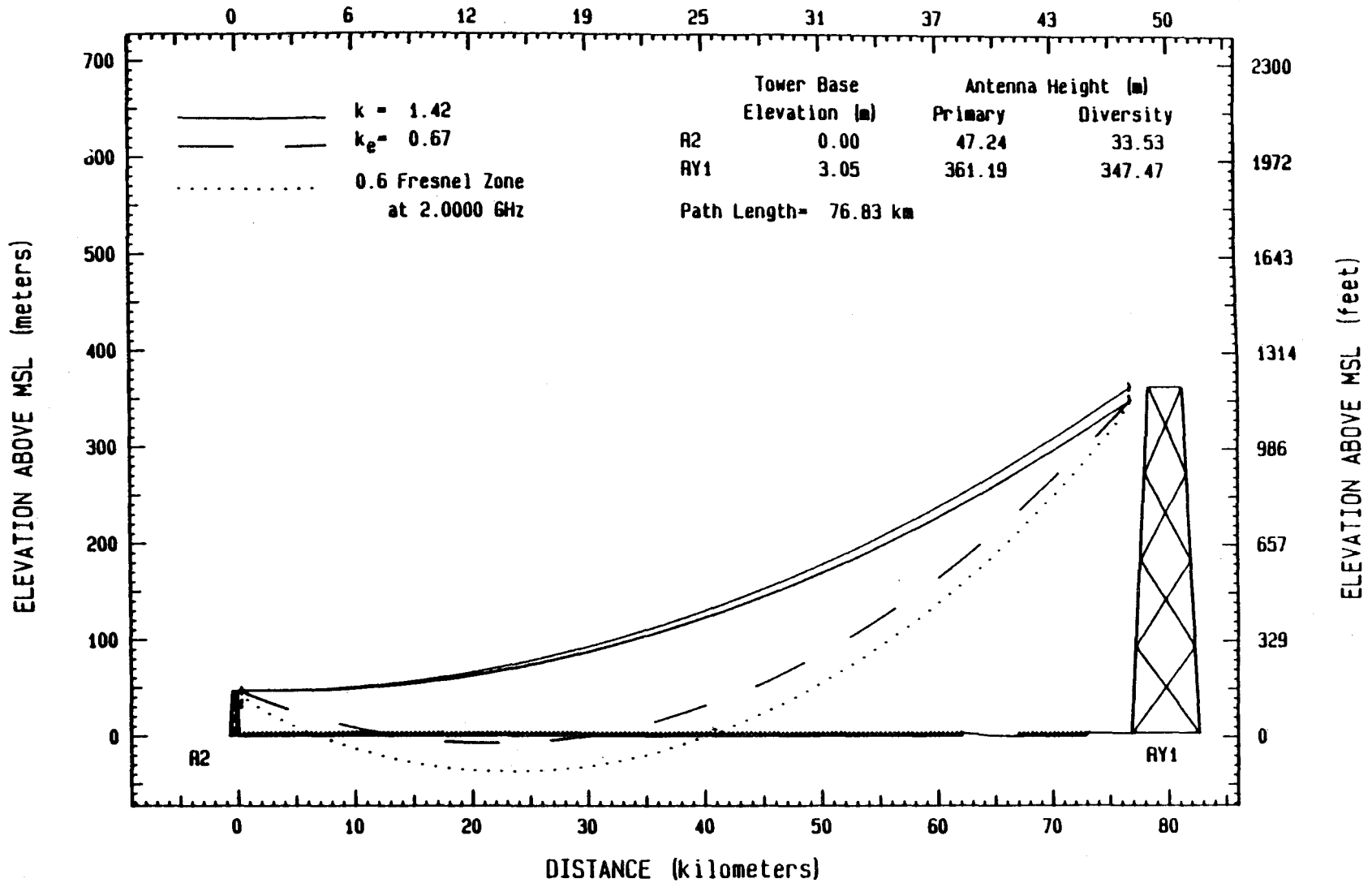
Figure A-1. Path profile for the multipath attenuation distribution calculation.

Single Receiver Basic Transmission Loss Due to Multipath   (dB)

140

150

160

170

180

.9   .5   .1   .01   .001   .0001   .00001

Fraction of Time that the Corresponding Multipath Basic Transmission Loss is Not Exceeded
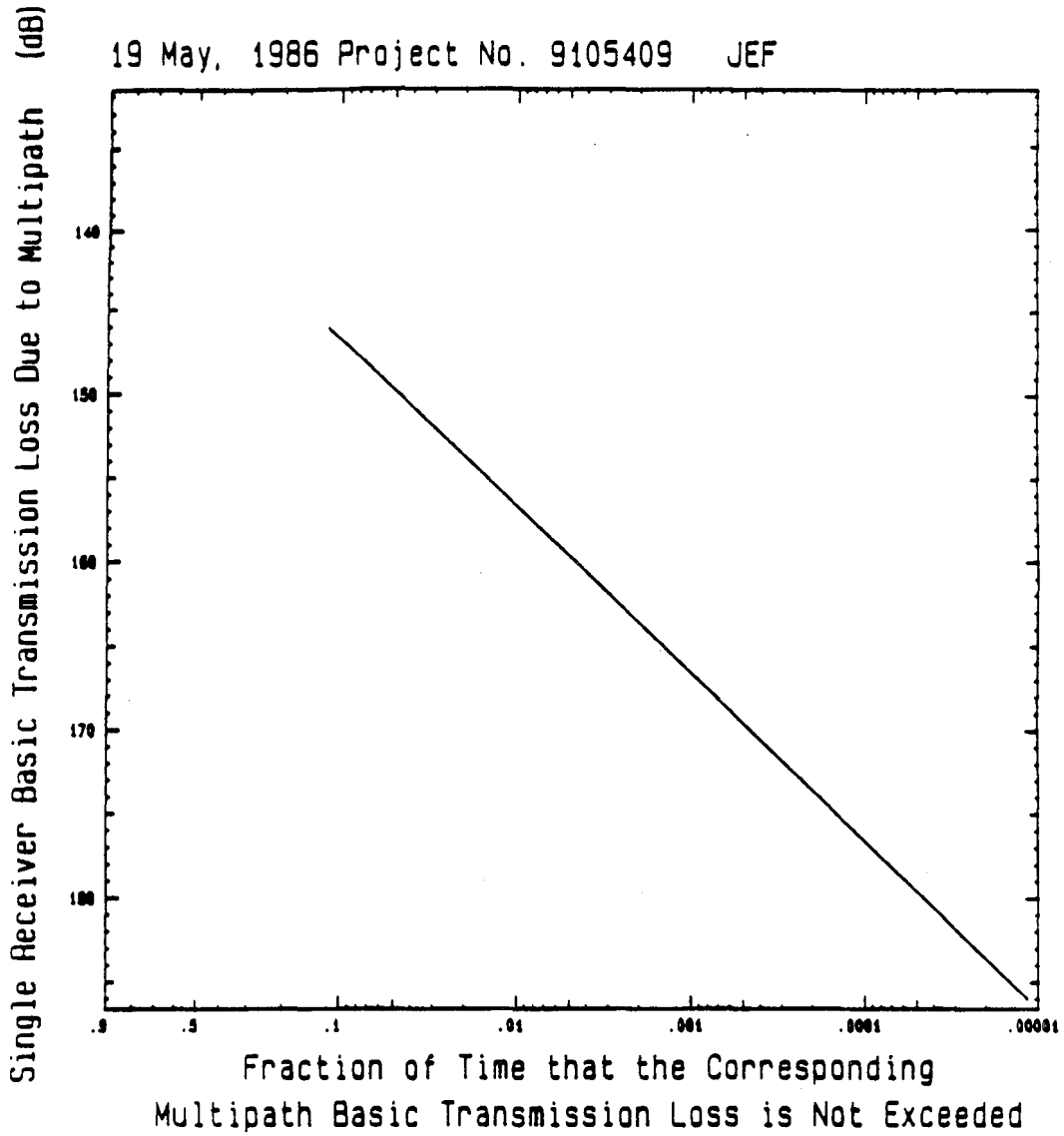
Path Length	km	76.827
Effective Path Length	km	76.827
Primary Frequency	GHz	2.000
Polarization		Vertical
Median Basic Transmission Loss	dB	136.640
Std Deviation of Terrain Elev	m	0.151
Average Annual Temperture	Celsius	19.722
Region		Coastal
Annual Occurance Factor		0.72163

Figure A-2.   Multipath attenuation distribution.

Table A-3. Carrier to Noise Probability Distribution Parameters

Carrier-to-Noise Probability Distribution Parameters
Ocean Tower R2 to Shore Tower

Path 1 Parameters - Ocean Tower R2 to Shore Tower

Path Length	(km)	76.827
Transmitter Antenna Type		Parabolic
Receiver Antenna Type		Parabolic
Transmitter Final Amplifier Type		Constant power
Primary Carrier Frequency	(GHz)	2.0000
Diversity Carrier Frequency	(GHz)	2.0000
Transmitter Antenna Gain	(dBi)	31.5734
Primary Receiver Antenna Gain	(dBi)	33.5116
Diversity Receiver Antenna Gain	(dBi)	33.5116
Site Loss on the Receiver End of the Path	(dB)	
Median Basic Transmission Loss Across the Path	(dB)	136.6395
Rain Attenuation for P=0.01	(dB)	0.0427
Rain Attenuation for P=0.001	(dB)	0.3550
Rain Attenuation for P=0.0001	(dB)	0.9695
Rain Attenuation for P=0.00001	(dB)	1.5048
Rain Radome Loss Due to Rain	(dB)	0.4000
Annual Multipath Fading Occurance Factor		0.7216
Diversity Type		Space
Vertical Diversity Spacing	(m)	13.716
Combiner Switching Threshold Power Ratio	(dB)	3.0000
Transmitter Feeder Line Length	(m)	50.2920
Transmitter Feeder Line Loss per 100 meters	(dB/100m)	1.8500
Transmitter Feeder Line Loss	(dB)	0.9304
Transmitter Diplexer Loss	(dB)	1.0000
Receiver Feeder Line Length	(m)	370.3320
Receiver Feeder Line Loss per 100 meters	(dB/100m)	1.8500
Receiver Feeder Line Loss	(dB)	6.8511
Receiver Diplexer Loss	(dB)	1.0000
Transmitter Final Amplifier Power Output	(dBm)	40.0000
Transmitter Power at the Antenna Terminals	(dBm)	38.0696
Receiver Noise Figure	(dB)	7.0000
Receiver Bandwidth	(MHz)	7.0000
Receiver Thermal Noise	(dBm)	-97.5490
Median Received Signal Level for the Path	(dBm)	-41.3362
Median Thermal C/N at the Receiver Output	(dB)	56.2128
Median C/N at the Transmitter	(dB)	60.0000
Median Path C/N at the Receiver Output	(dB)	54.6958

Table A-4. Digital Link Performance Parameters

19 May, 1986 Project:9105409 JEF

PCM-TDM Performance Parameters
Ocean Tower R2 to Shore Tower

Total Length of the Link	(km)	76.8268
Data Transmission Rate	(Mb/s)	6.300
Modulation Type		QPSK
Mfg Bit-Error-Rate Threshold	(dBm)	-79.00
Mfg Bit-Error-Rate at Threshold		0.0000000
Median Received C/N	(dB)	54.696
Median Received Signal Level	(dBm)	-41.336
Outage Bit-Error-Rate		0.00000100
Threshold Received C/N	(dB)	15.012
Fade Margin	(dB)	39.684
Desired Error-Free-Second Availability		0.99999520
Calculated Error-Free-Second Availability		0.99999910
Is Performance Satisfactory?		No

Note: These values cover propagation effects, not equipment outages.
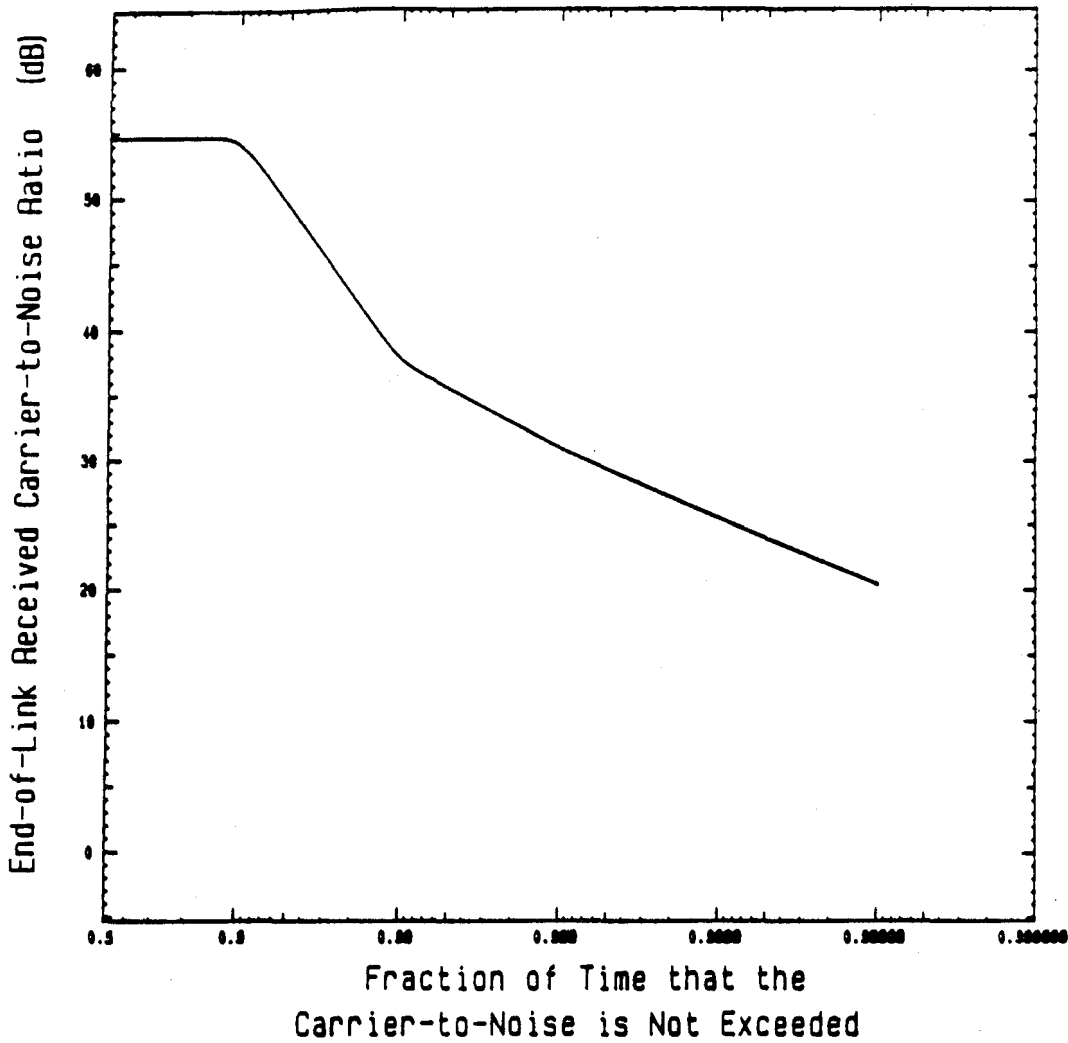
31

Figure A-3. Link pre-detection carrier-to-noise ratio distribution.

PERCENT OF TIME ORDINATE IS NOT EXCEEDED

Cumulative Distribution of the
Observed Radio Refractivity Gradient
in the Ground-based 100-meter Layer

CAPE HATTERAS

——— February   — — — May
—·—·— August   ·········· November

PERCENT OF TIME ORDINATE IS EXCEEDED
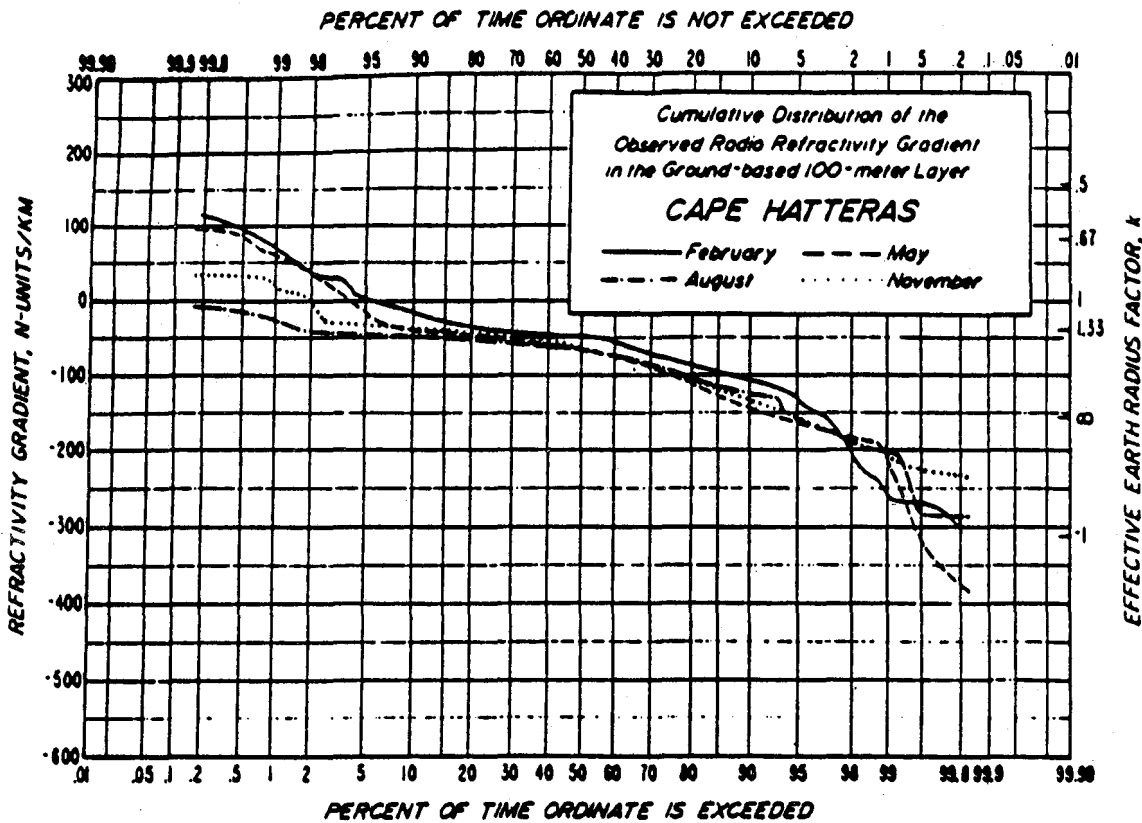
Cape Hatteras, N. Carolina

35° 16' N, 75° 33' W   3 m m.s.l.

Data: Radiosonde.   0300 and 1500Z (2200 and 1000 LST):   8/52 - 5/57

Temperature (°F):   January 53/40; July 84/72

Mean Dewpoint (°F):   Not available

Precipitation (inches): Annual 54.5; August 6.42; April 2.99

Located on an elongated sandy island in the Outer Banks of North Carolina.
The Gulf Stream of the Atlantic Ocean passes 30 to 80 km offshore. A
maritime climate with warm summers and cool winters. Relatively windy.

Figure A-4. Measured refractivity gradient distribution.

33

Table A-5. Bi-Modal Refractivity Gradient Distribution Parameters

Refractivity Gradient Distribution Parameters
Ocean Tower R2 to Shore Tower

Name	Units	Value
Annual Mean Refractivity Gradient	n-units/km	-52.00000
Layer Thickness	m	100.00000
Region		Coastal
Probability of a Temp Inversion		0.30000
Air Horizontal Homogeneity		1.00000
Dist to a Large Body of Water	km	0.00000
Wind Direction Factor		0.20000
Average Temperature	Celsius	19.72222
Mean Annual Precipitation	mm	1400.00000
Surface Moisture Index		23.43889
Water Proximity Factor		1.00000
Water Vapor Capacity		0.47195
Surface Moisture Factor		0.21404
Mixed Regime Std Deviation	n-units/km	15.00000
Stratified Regime Std Deviation	n-units/km	91.42112

Refractivity Gradient and Earth's Radius Factor Distributions:

Probability, q That the N' Value Is Exceeded	Refractivity Gradient, N' (n-units/km)	Earth's Radius Factor, k
.9	-71.13910	1.82868
.5	-50.37694	1.47254
.1	-10.45983	1.07139
.01	64.35218	0.70926
.001	131.72485	0.54375
.0001	188.78524	0.45402
.00001	238.58537	0.39686
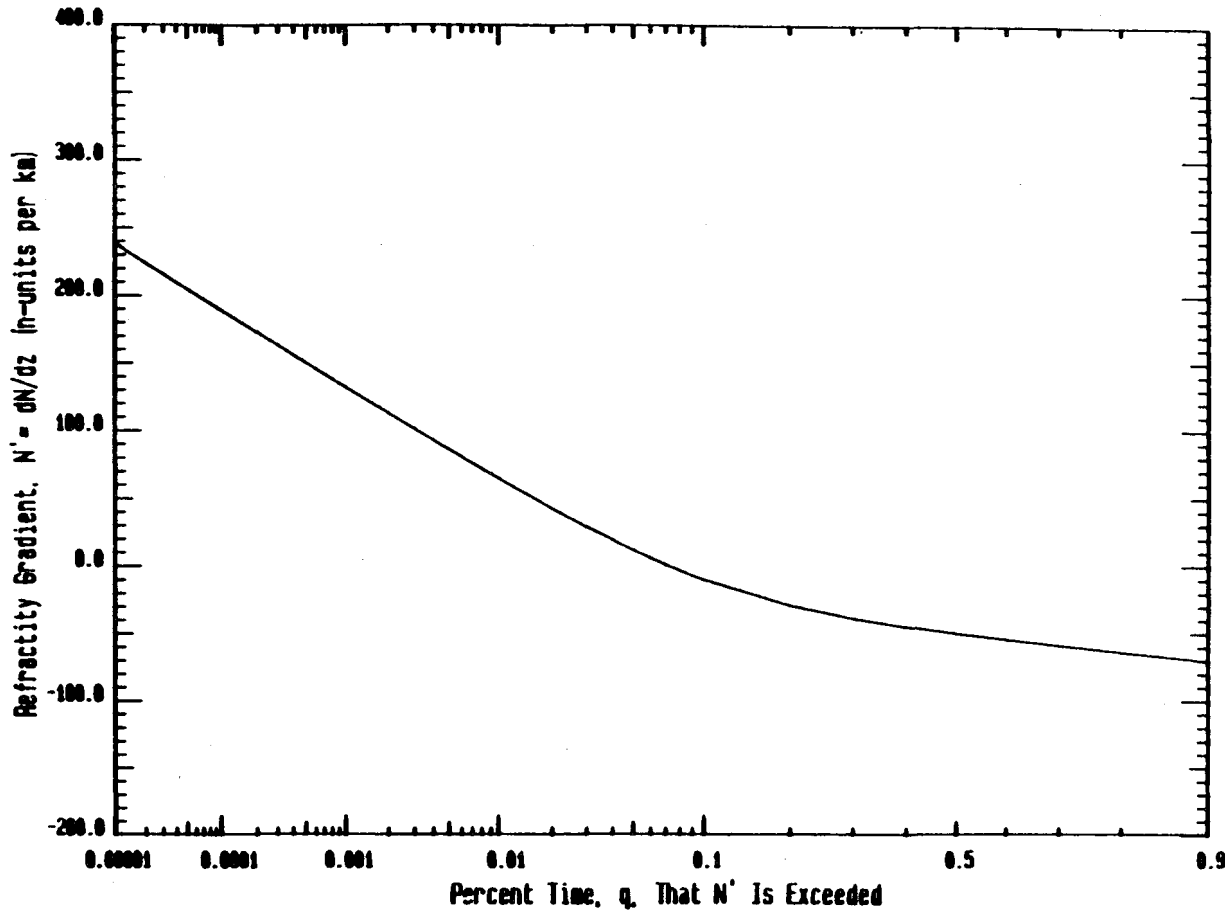
Region:
    Coastal
Air Horizontal Homogeneity:
    1.000
Probability of Temp Inversion:
    0.300
Wind Direction Factor:
    0.200
Average July Temperature:
    26.667 degrees Celsius
Average January Temperature:
    12.778 degrees Celsius
Surface Moisture Index:
    23.439
Distance to a Large Body of Water:
    0.000
Annual Mean Refractity Gradient:
    52.000 n-units per km

Refractity Gradient Distribution
Ocean Tower R2 to Shore Tower Path

Figure A-5. Calculated bi-modal refractivity gradient distribution.

DISTANCE (miles)

19 May, 1985 Project 9105409 JEF

	0.00	6.22	12.43	18.65	24.86	31.08	37.29	43.51

	Latitude	Longitude	Elev (m)	Antenna Height Primary	Diversity	Azimuth to Other Site True North	Magnetic	Take-off Angle
R2	31 22' 28.9"N	80 33' 59.5"W	0.0	47 m	34 m	286 58' 48.4"	286 58' 48.4"	00' 07.0"
RY1	31 34' 30.0"N	81 20' 26.0"W	3.0	361 m	347 m	106 34' 33.4"	106 34' 33.4"	-28' 15.1"

Path Length = 76.83 km

q = 0.5

k = 1.4725

0.6 of 1st Fresnel Zone

ELEVATION (meters)

ELEVATION (feet)

550 — 1804
500 — 1640
450 — 1476
400 — 1312
350 — 1148
300 — 984
250 — 820
200 — 656
150 — 492
100 — 328
50 — 164
0 — 0

R2

RY1

Mean Sea Level

DISTANCE (kilometers)

| 0 | 10 | 20 | 30 | 40 | 50 | 60 | 70 | 80 |

Figure A-6.   Ray path for probability of 0.5 corresponding to k=1.472.

DISTANCE (miles)

19 May, 1986 Project 9105409 JEF

	Latitude	Longitude	Elev (m)	Antenna Height Primary	Diversity	Azimuth to Other Site True North	Magnetic	Take-off Angle
A2	31 22' 28.8"N	80 33' 58.5"W	0.0	47 m	34 m	286 58' 48.4°	286 58' 48.4°	-05' 08.0°
RY1	31 34' 38.0"N	81 20' 25.0"W	3.0	361 m	347 m	106 34' 33.4°	106 34' 33.4°	-33' 31.1°

Path Length = 76.83 km

q = 0.1

k = 1.0714

0.6 of 1st Fresnel Zone

RY1

Mean Sea Level

A2

ELEVATION (meters)

ELEVATION (feet)

DISTANCE (kilometers)

Figure A-7. Ray path for probability of 0.1 corresponding to k=1.071.

Figure A-8. Ray path for probability of 0.01 corresponding to k=0.709.

19 May, 1986 Project 9105409 JEF

	Latitude	Longitude	Elev (m)	Antenna Height Primary	Diversity	Azimuth to Other Site True North	Magnetic	Take-off Angle
R2	31 22' 29.9"N	80 33' 59.5"W	0.0	47 m	34 m	286 58' 48.4°	286 58' 48.4°	-17' 56.8°
RY1	31 34' 30.0"N	81 20' 26.0"W	3.0	361 m	347 m	106 34' 33.4°	106 34' 33.4°	-49' 50.2°

Path Length = 76.83 km
q = 0.001
k = 0.5437

Mean Sea Level

R2

RY1

ELEVATION (meters)

ELEVATION (feet)

DISTANCE (kilometers)

39
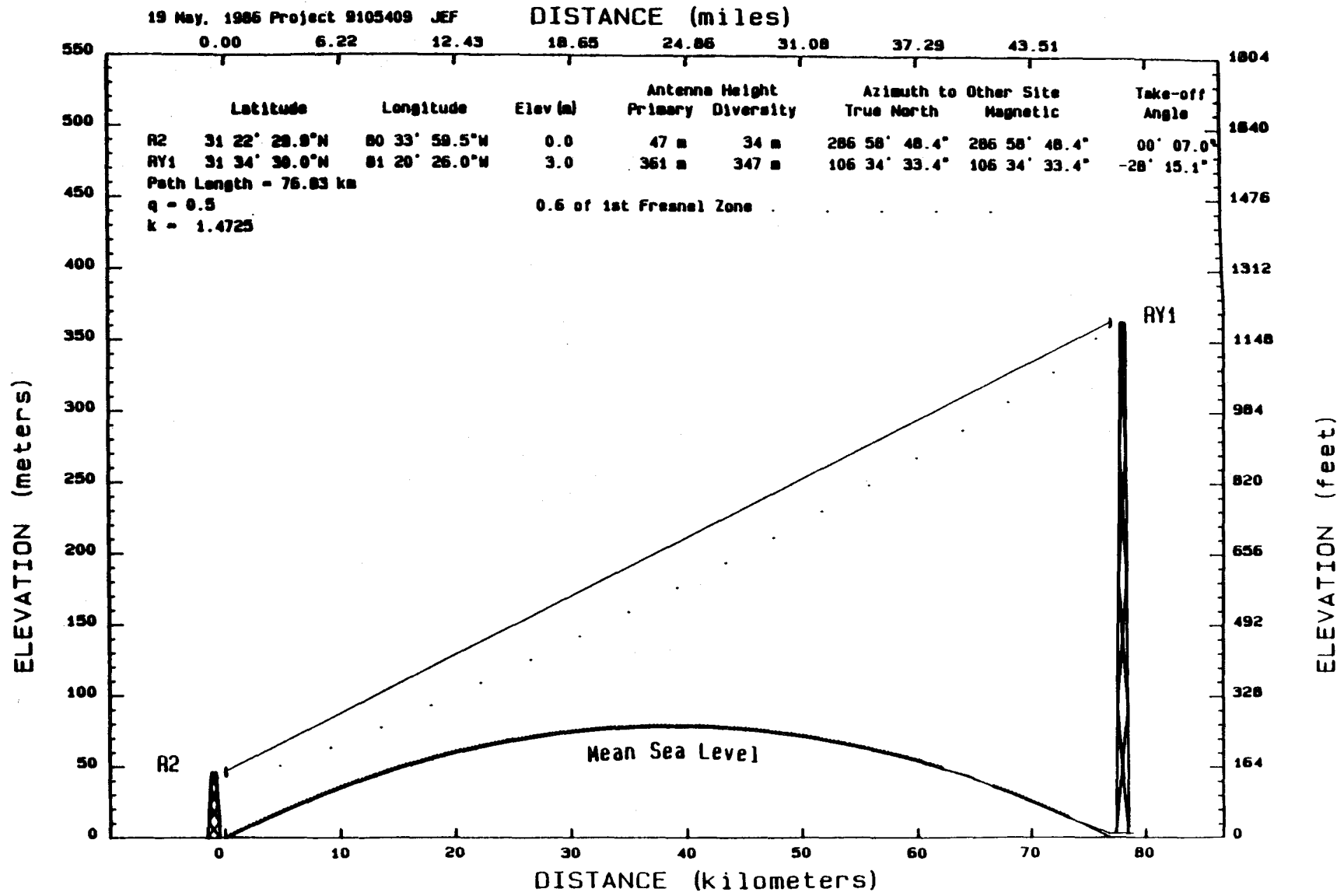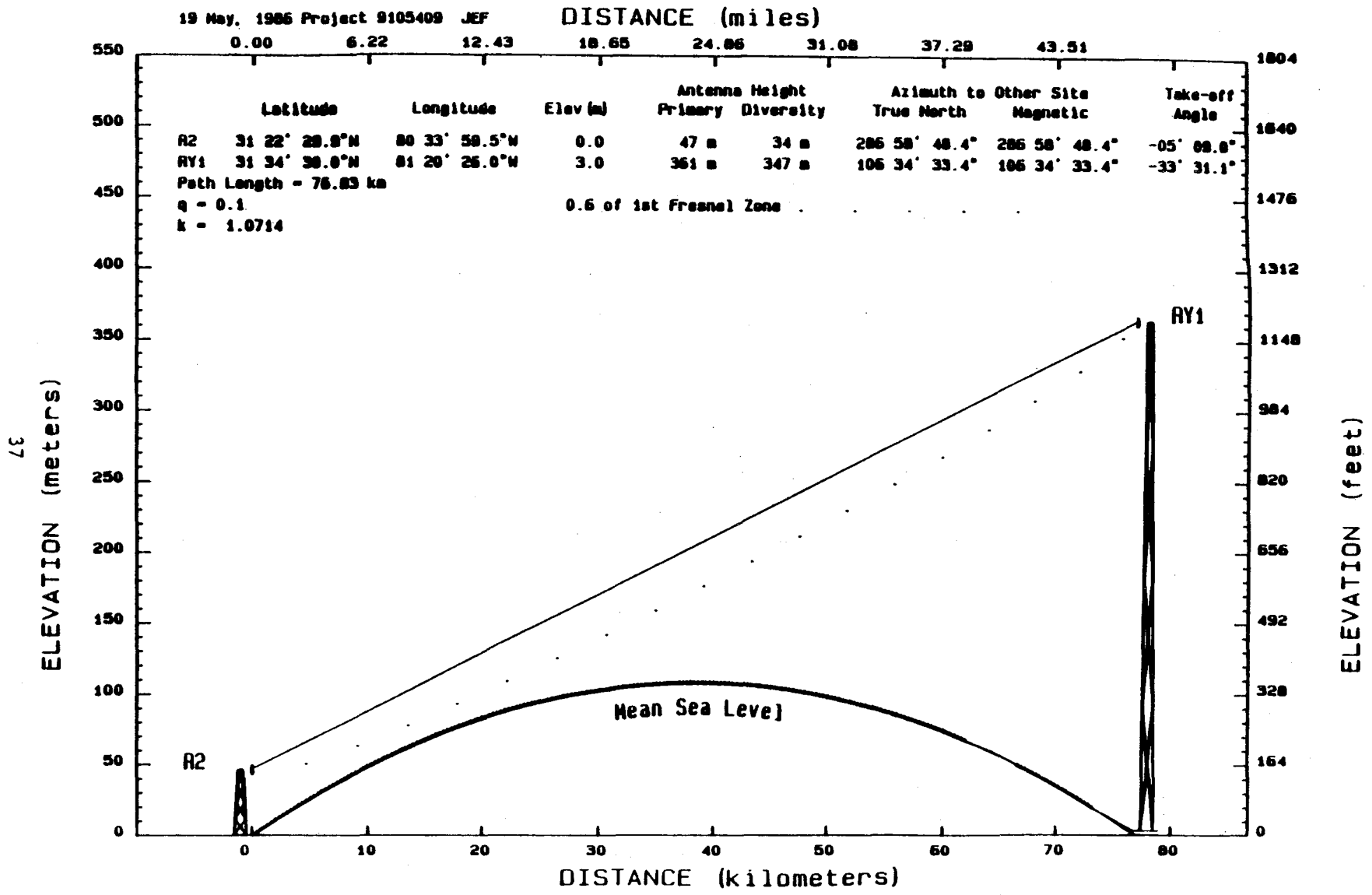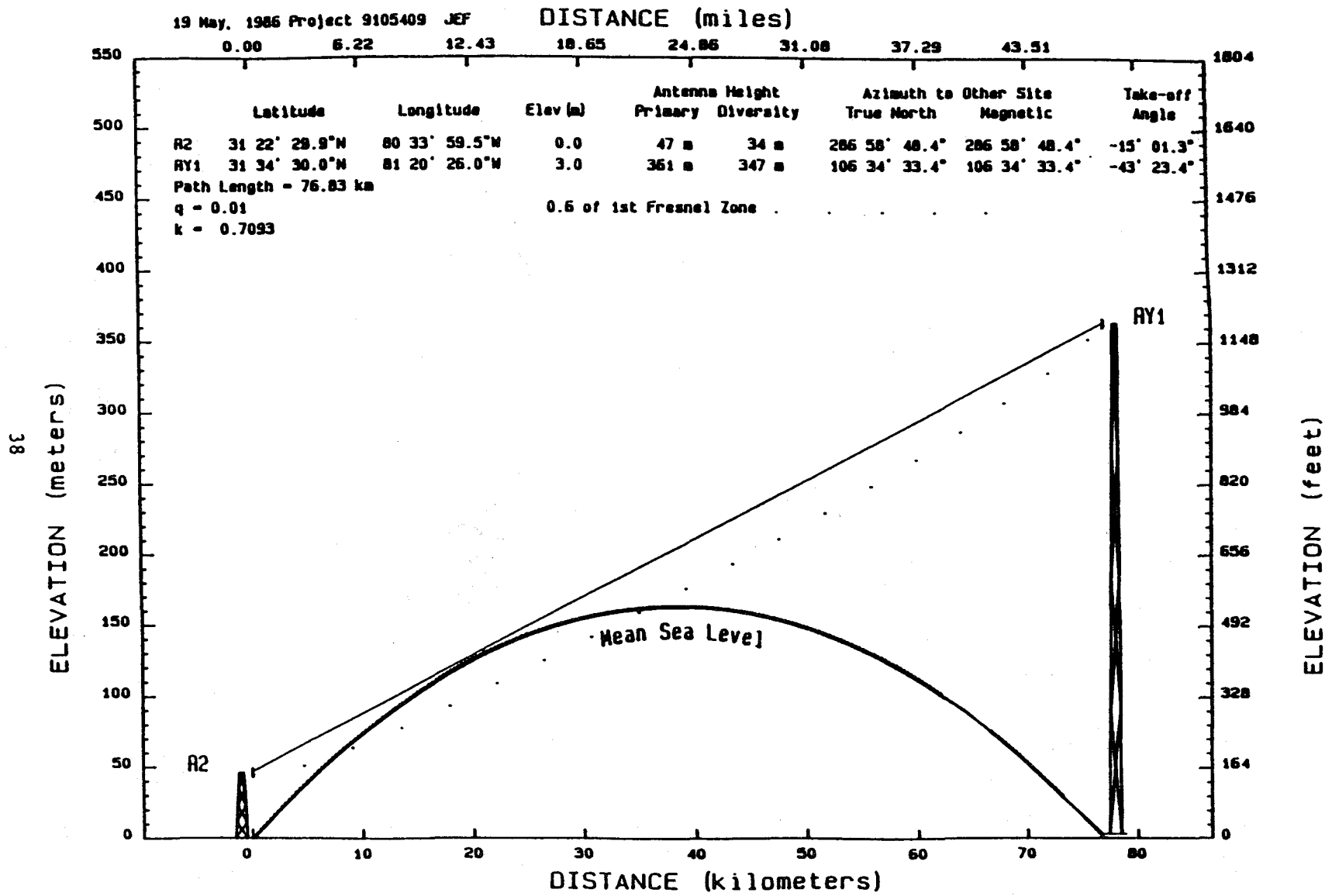
Figure A-9. Ray path for probability of 0.001 corresponding to k=0.544.

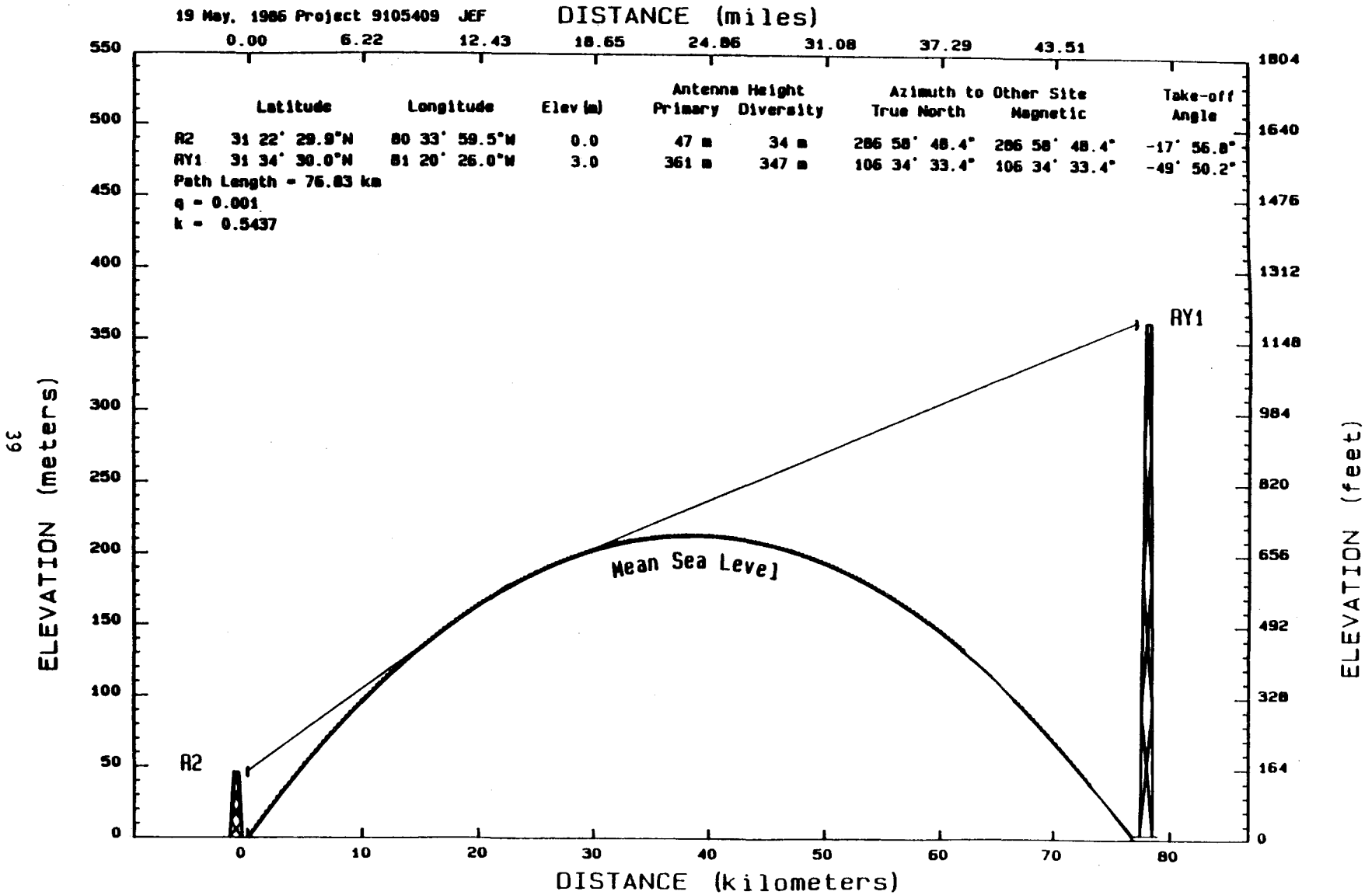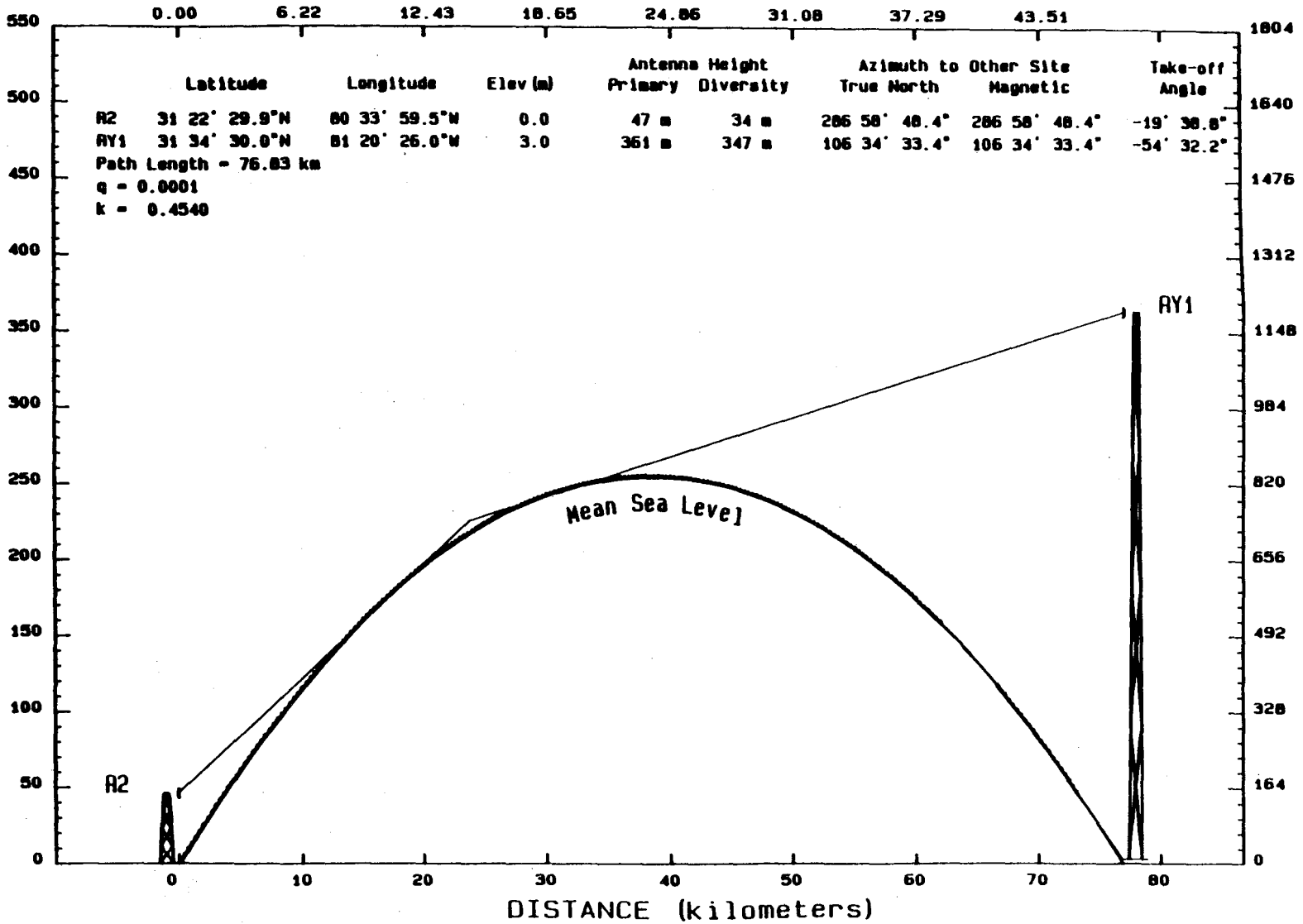Figure A-10. Ray path for probability of 0.0001 corresponding to k=0.454.

DISTANCE (miles)

0.00   6.22   12.43   18.65   24.86   31.08   37.29   43.51

	Latitude	Longitude	Elev (m)	Antenna Height Primary	Antenna Height Diversity	Azimuth to Other Site True North	Azimuth to Other Site Magnetic	Take-off Angle
R2	31 22' 29.9"N	80 33' 59.5"W	0.0	47 m	34 m	286 58' 48.4"	286 58' 48.4"	-21' 00.9"
RY1	31 34' 30.0"N	81 20' 26.0"W	3.0	361 m	347 m	106 34' 33.4"	106 34' 33.4"	-58' 19.8"

Path Length = 76.83 km

q = 0.00001

k = 0.3969

RY1

Mean Sea Level

R2

ELEVATION (meters)

ELEVATION (feet)

DISTANCE (kilometers)

Figure A-11.   Ray path for probability of 0.00001 corresponding to k=0.370.

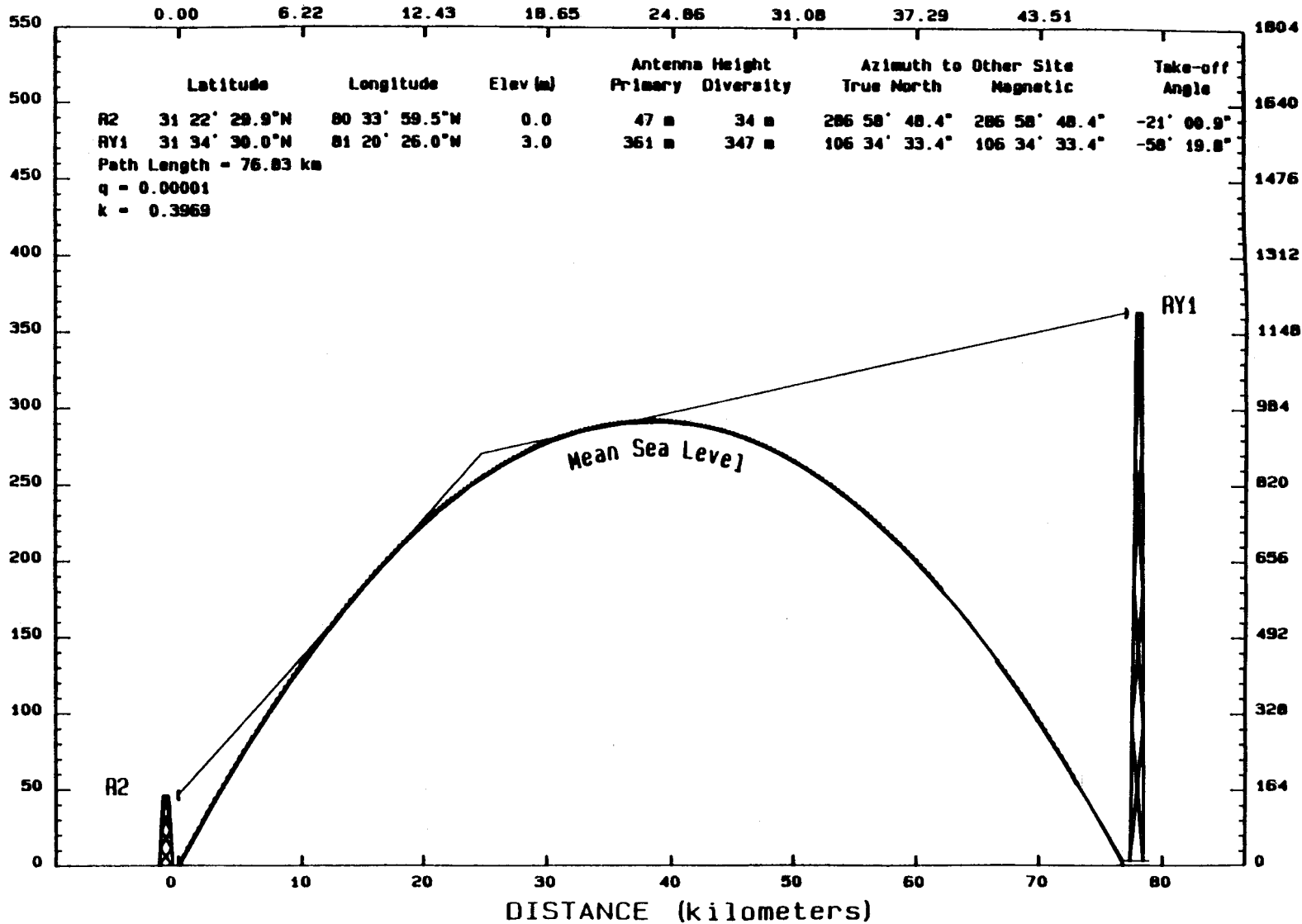Table A-6. Dominant Mode Determination and Transmission Loss Distribution

Dominant Mode and Combined Loss
Ocean Tower R2 to Shore Tower

This path is line-of-sight with marginal clearance.

Variables Independent of Refractivity Gradient:

Path Length	(km)	76.827
Primary Frequency	(MHz)	2000.000
R2 Transmitter Antenna Diameter	(m)	2.438
RY1 Receiver Antenna Diameter	(m)	3.048
Diversity Antenna Diameter	(m)	3.048
R2 Transmitter Antenna Gain	(dBi)	31.573
RY1 Receiver Antenna Gain	(dBi)	33.512
Diversity Antenna Gain	(dBi)	33.512
Line-of-sight Basic Transmission Loss	(dB)	136.639

Variables Dependent Upon Refractivity Gradient:

Cumulative Probability q	Obst. Diffr. Basic Transmission Loss (dB)	Total Antenna Pointing Loss (dB)	Minimum Clearance (1st Fresnel Radii)	Smooth Earth Diffraction Basic Trans. Loss (dB)	Tropospheric Scatter Basic Trans. Loss (dB)
0.9	136.63846	0.00175	1.62448		152.18846
0.5	136.63941	0.00000	1.40532		152.18941
0.1	136.64124	0.00648	0.96472		152.19124
0.01	143.86561	0.05361	0.08682		152.19470
0.001	161.68209	0.09634	-0.74211	164.37817	168.33600
0.0001	175.94544	0.13447	-1.46372	173.17841	178.98848
0.00001	188.72544	0.17032	-2.10369	182.55694	184.68116

Cumulative Probability q	Antenna To Medium Coupling Loss (dB)	R2 Antenna Pointing Loss (dB)	RY1 Antenna Pointing Loss (dB)	Combined Basic Trans. and Pointing Loss (dB)	Dominant Mode
0.9	2.33346	0.00110	0.00172	136.64021	Line of Sight
0.5	2.33346	0.00000	0.00000	136.63941	Line of Sight
0.1	2.33346	0.00407	0.00637	136.64772	Line of Sight
0.01	2.33346	0.03368	0.05265	143.91921	Obstacle Diff
0.001	2.33346	0.04798	0.10717	163.55821	Smooth Earth
0.0001	2.33346	0.05744	0.15911	172.69332	Smooth Earth
0.00001	2.33346	0.06568	0.20860	181.39734	Smooth Earth
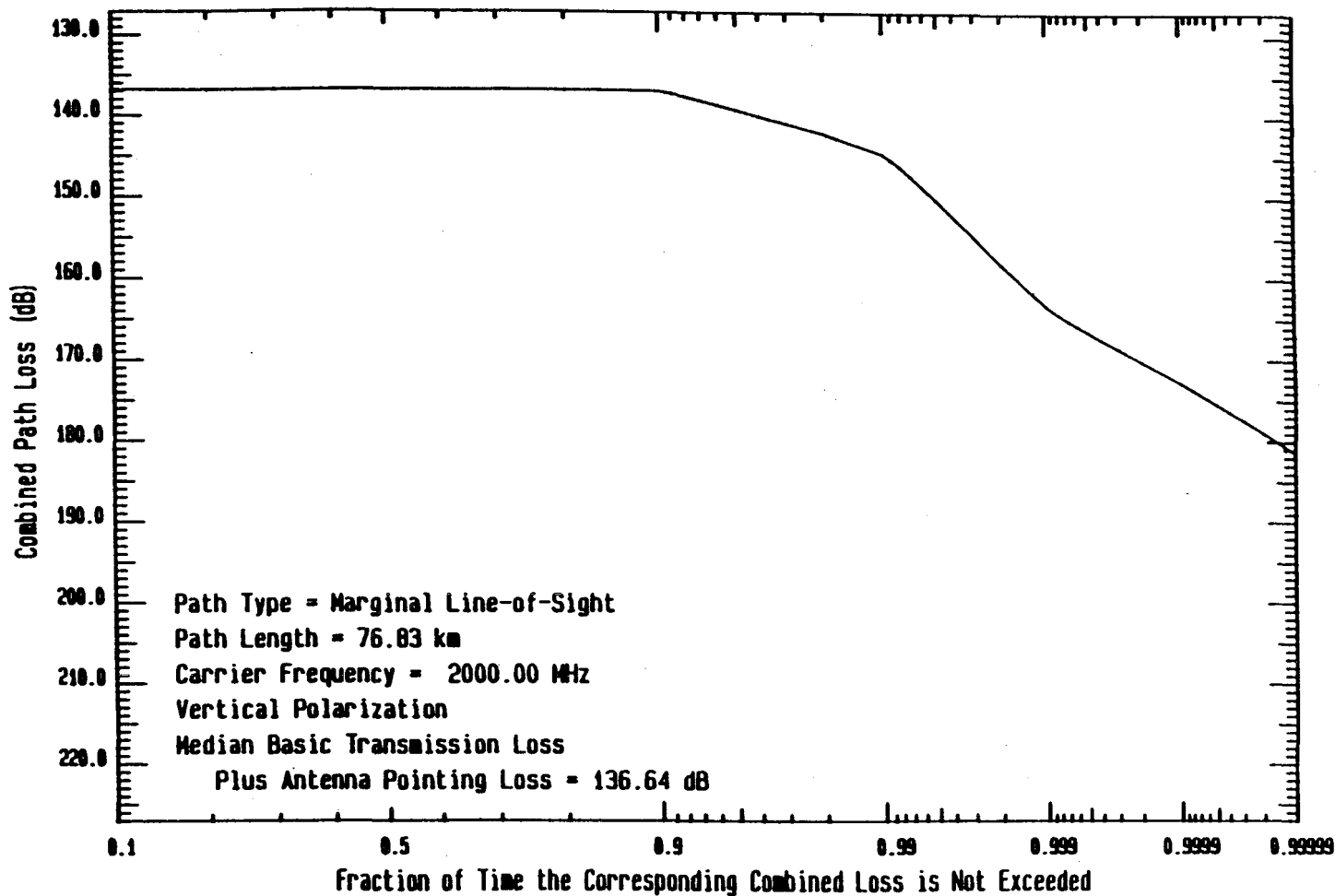
Long-Term Combined Loss Distribution
Ocean Tower R2 to Shore Tower Path

Figure A-12. Mixed mode combined long-term path loss distribution.

43

FORM NTIA-29
(4-80)

U.S. DEPARTMENT OF COMMERCE
NAT'L. TELECOMMUNICATIONS AND INFORMATION ADMINISTRATION

BIBLIOGRAPHIC DATA SHEET

	1. PUBLICATION NO.	2. Gov't Accession No.	3. Recipient's Accession No.

4. TITLE AND SUBTITLE	5. Publication Date
Design and Performance of a Long, Over-Water Microwave Radio Link	February 1990
	6. Performing Organization Code
	NTIA/ITS

7. AUTHOR(S)	9. Project/Task/Work Unit No.
Joseph E. Farrow	

8. PERFORMING ORGANIZATION NAME AND ADDRESS	
National Telecommunications & Information Administration Institute for Telecommunication Sciences 325 Broadway Boulder, CO 80303	10. Contract/Grant No.

11. Sponsoring Organization Name and Address	12. Type of Report and Period Covered
Naval Air Test Center Commander Patuxent River, MD 20670-5304	
	13.

14. SUPPLEMENTARY NOTES

15. ABSTRACT *(A 200-word or less factual summary of most significant information. If document includes a significant bibliography or literature survey, mention it here.)*

This paper discusses the design and the measured performance of a 76.8-km (47.7-mi) over-water 2.3 GHz microwave radio link. Since one of the terminals was located on an ocean tower, the maximum antenna height at that location was restricted to 49 m (160 ft). A 367-m (1200 ft) tower was used at the shore end to provide ray path clearance for normal and extreme refractivity gradients. The tower at the shore end supported antennas at 361 m (1180 ft), 345 m (1128 ft), 229 m (750 ft), and 49 m (160 ft) to provide quadruple diversity protection. Received signal level measurements were made over the link for several months including some of the summer period. Propagation performance of the link during this period was satisfactory.

16. Key Words *(Alphabetical order, separated by semicolons)*

2 GHz propagation; long over-water path; quadruple diversity performance analysis; refractive gradient analysis

17. AVAILABILITY STATEMENT	18. Security Class. *(This report)*	20. Number of pages
☒ UNLIMITED.	Unclassified	44
	19. Security Class. *(This page)*	21. Price:
☐ FOR OFFICIAL DISTRIBUTION.	Unclassified	